NAVAL POSTGRADUATE SCHOOL

MONTEREY, CALIFORNIA

THESIS

COMBUSTION HEAT RELEASE RATE COMPARISON OF ALGAE HYDROPROCESSED RENEWABLE DIESEL TO F-76 IN A TWO-STROKE DIESEL ENGINE

by

John H. Petersen

June 2013

Thesis Advisor:	Knox T. Millsaps
Co-Advisor:	Douglas L. Seivwright
Second Reader:	Patrick A. Caton

THIS PAGE INTENTIONALLY LEFT BLANK

REPORT DOCUMENTATION PAGE			Form Approved OMB No. 0704-0188
Public reporting burden for this collection of information is estimated to average 1 hour per response, including the time for reviewing instruction, searching existing data sources, gathering and maintaining the data needed, and completing and reviewing the collection of information. Send comments regarding this burden estimate or any other aspect of this collection of information, including suggestions for reducing this burden, to Washington headquarters Services, Directorate for Information Operations and Reports, 1215 Jefferson Davis Highway, Suite 1204, Arlington, VA 22202-4302, and to the Office of Management and Budget, Paperwork Reduction Project (0704-0188) Washington DC 20503.			
1. AGENCY USE ONLY ***(Leave blank)***	**2. REPORT DATE** June 2013	**3. REPORT TYPE AND DATES COVERED** Master's Thesis	
4. TITLE AND SUBTITLE COMBUSTION HEAT RELEASE RATE COMPARISON OF ALGAE HYDROPROCESSED RENEWABLE DIESEL TO F-76 IN A TWO-STROKE DIESEL ENGINE			**5. FUNDING NUMBERS**
6. AUTHOR(S) John H. Petersen			
7. PERFORMING ORGANIZATION NAME(S) AND ADDRESS(ES) Naval Postgraduate School Monterey, CA 93943-5000			**8. PERFORMING ORGANIZATION REPORT NUMBER**
9. SPONSORING /MONITORING AGENCY NAME(S) AND ADDRESS(ES) Office of Naval Research			**10. SPONSORING/MONITORING AGENCY REPORT NUMBER**
11. SUPPLEMENTARY NOTES The views expressed in this thesis are those of the author and do not reflect the official policy or position of the Department of Defense or the U.S. Government. IRB Protocol number ____N/A____.			
12a. DISTRIBUTION / AVAILABILITY STATEMENT Approved for public release; distribution is unlimited			**12b. DISTRIBUTION CODE**

13. ABSTRACT (maximum 200 words)

This thesis compared the combustion performance of algae-based hydroprocessed renewable Diesel fuel (HRD) and HRD/F-76 blends, to that of conventional Naval Diesel fuel, F-76. The tests were conducted using a two-stroke, direct injected Detroit 3-53 Diesel engine. The cetane number (CN) of the HRD used was 78 while the CN of the F-76 used was 46. The start of injection (SOI) was measured with a strain gauge mounted on the mechanical fuel injector rocker arm. SOI was found to advance as load increased and retard as speed increased; however, SOI remained constant with the use of the different fuels HRD or F-76. Ignition delay (IGD) decreased significantly with HRD which is consistent with the much higher CN. The heat release rate analysis performed determined that the shorter IGD of HRD led to later combustion phasing, increased overall combustion duration and lower maximum rate of pressure rise. The use of HRD also resulted in lower max cylinder pressure. These results suggest that the combustion performance of HRD has no detrimental effects on the Diesel engine tested.

14. SUBJECT TERMS Hydroprocessed Renewable Diesel, HRD, Algae Derived Alternative Fuels, Bio-derived Fuels, Renewable Diesel, Alternative Fuel Blends, HVO, F-76, Heat Release Rate, Energy Release Rate, Diesel Engine Combustion			**15. NUMBER OF PAGES** 103
			16. PRICE CODE
17. SECURITY CLASSIFICATION OF REPORT Unclassified	**18. SECURITY CLASSIFICATION OF THIS PAGE** Unclassified	**19. SECURITY CLASSIFICATION OF ABSTRACT** Unclassified	**20. LIMITATION OF ABSTRACT** UU

NSN 7540-01-280-5500 Standard Form 298 (Rev. 2-89)
Prescribed by ANSI Std. 239-18

THIS PAGE INTENTIONALLY LEFT BLANK

Approved for public release; distribution is unlimited

COMBUSTION HEAT RELEASE RATE COMPARISON OF ALGAE HYDROPROCESSED RENEWABLE DIESEL TO F-76 IN A TWO-STROKE DIESEL ENGINE

John H. Petersen
Lieutenant, NOAA Commissioned Officer Corps
B.S., California Polytechnic State University, San Luis Obispo, 2007

Submitted in partial fulfillment of the
requirements for the degree of

MASTER OF SCIENCE IN MECHANICAL ENGINEERING

from the

NAVAL POSTGRADUATE SCHOOL
June 2013

Author: John H. Petersen

Approved by: Knox T. Millsaps
Thesis Advisor

Douglas L. Seivwright
Thesis Co-Advisor

Patrick A. Caton
Second Reader

Knox T. Millsaps
Chair, Department of Mechanical and Aerospace Engineering

THIS PAGE INTENTIONALLY LEFT BLANK

ABSTRACT

This thesis compared the combustion performance of algae-based hydroprocessed renewable Diesel fuel (HRD) and HRD/F-76 blends, to that of conventional Naval Diesel fuel, F-76. The tests were conducted using a two-stroke, direct injected Detroit 3-53 Diesel engine. The cetane number (CN) of the HRD used was 78 while the CN of the F-76 used was 46. The start of injection (SOI) was measured with a strain gauge mounted on the mechanical fuel injector rocker arm. SOI was found to advance as load increased and retard as speed increased; however, SOI remained constant with the use of the different fuels HRD or F-76. Ignition delay (IGD) decreased significantly with HRD which is consistent with the much higher CN. The heat release rate analysis performed determined that the shorter IGD of HRD led to later combustion phasing, increased overall combustion duration and lower maximum rate of pressure rise. The use of HRD also resulted in lower max cylinder pressure. These results suggest that the combustion performance of HRD has no detrimental effects on the Diesel engine tested.

THIS PAGE INTENTIONALLY LEFT BLANK

TABLE OF CONTENTS

LIST OF FIGURES

LIST OF TABLES

THIS PAGE INTENTIONALLY LEFT BLANK

LIST OF ACRONYMS AND ABBREVIATIONS

AOP	Angle of peak (degrees)
ATC	After top center
bpd	Barrels per day
BTC	Before top center
CAD	Crank angle degrees
CAD10	CAD corresponding to 10% mass fraction burned point
CAD50	CAD corresponding to 50% mass fraction burned point
CAD90	CAD corresponding to 90% mass fraction burned point
CD	Combustion duration
CFR	Cooperative Fuels Research
CI	Compression ignition
CN	Cetane number
CP	Combustion phasing
D2	Number 2 Diesel fuel
DAQ	Data acquisition
DoD	Department of Defense
DoN	Department of Navy
EVC	Exhaust valve closed
EVO	Exhaust valve open
FAME	Fatty acid methyl esters
FT	Fischer-Tropsch
$h_C = \frac{\delta Q_H}{A(T_{CG} - T_W)}$	Heat transfer coefficient
HRD	Hydroprocessed renewable Diesel
HRJ	Hydroprocessed renewable jet fuel
HMMWV	High Mobility Multipurpose Wheeled Vehicle
HVO	Hydroprocessed vegetable oil
IGD	Ignition delay
IPC	Intake ports closed

IPO	Intake ports open
K	Kelvin
$k = \frac{C_p}{C_V}$	Ratio of specific heats (1)
kg	Kilogram
L	Liter
m	Mass (kg)
M	Molar mass (kg/mol)
mL	Milliliter
MPL	Marine Propulsion Lab
ms	milliseconds
NATO	North Atlantic Treaty Organization
NAVAIR	Naval Air Systems Command
NPS	Naval Postgraduate School
ONR	Office of Naval Research
PP	Peak pressure
$R_{spec} = \frac{R}{M}$	Specific gas constant (J/kg·K)
SOC	Start of combustion
SOI	Stat of injection
SOP	Standard operating procedure
SwRI	Southwest Research Institute
t	Time
T	Temperature
TC	Top center
USN	United States Navy
USNA	United States Naval Academy
VI	Virtual instrument

ACKNOWLEDGMENTS

Thank you to my thesis advisors Dr. Knox Millsaps, Douglas Seivwright, and Dr. Patrick Caton for their feedback, support and ideas. I truly appreciate all the time and effort you invested in me. This whole experience was invaluable and I will continue draw from it throughout my life.

A special thanks to John Mobley and Levi Owen for their mechanical genius and willingness to accommodate my many impromptu requests. Your creativity saved me a tremendous amount of time.

I would also like to thank the ONR sponsors, specifically Dr. Sharon Beermann-Curtin, for providing me the opportunity to learn about biofuel combustion and to add to this exciting field of study. Without the support and supply of fuel from Sherry Williams at NAVAIR this research would not have been possible, thank you.

Lastly I would like to thank my patient, supportive, and eagle eyed wife. Without her meal deliveries, proof reading abilities and encouragement I would have been hungry, incorrectly phrased, and overwhelmed.

THIS PAGE INTENTIONALLY LEFT BLANK

I. INTRODUCTION

A. BACKGROUND

Petroleum products comprise 33% of our nation's total energy usage [1] and the U.S. uses 18.8 million barrels of petroleum every day. Even with technological advancements leading to improvements in fuel economy and public awareness on conservation, the Annual Energy Outlook of 2013 predicts our petroleum consumption levels to be the same in 2040 as they are today [2]. Due to the finite supply of fossil fuels, alternative and renewable energy resources may need to represent a large percentage of future energy consumption.

The U.S. currently imports 45% of its crude oil [1]. The Department of Defense (DoD) is the single largest consumer of energy in our nation [3], using approximately two percent of the U.S. petroleum demand, amounting to 337,000 barrels per day (bpd). The Navy itself uses 46,000 bpd of Naval Diesel fuel (NATO F-76) to power ships and land vehicles and 47,000 bpd of Naval jet fuel (JP-5) to fuel its aircraft. This large dependence on foreign oil jeopardizes energy security, possibly affecting the Navy's war fighting capability. "Our energy security is potentially subject to uncertainties that could impact the operations of the Navy and Marine Corps assets."[4]

In 2009, the Secretary of the Navy (SECNAV) outlined the following energy goals [5]:

- Sail Great Green Fleet by 2016, a Carrier Strike Group fueled by alternative power. Successful operation was demonstrated by the Green Strike Group during RIMPAC 2012.
- Reduce non-tactical petroleum use in the Navy's commercial fleet 50% by 2015.
- Increase alternative energy ashore: By 2020, 50% of the Navy's shore based energy will come from alternative sources and 50% of Navy and Marine Corps installations will be energy net-zero.
- Increase alternative energy Navy wide: By 2020, 50% of total energy of consumed will come from alternative sources.

To meet these goals, the Navy has implemented a program utilizing renewable biofuel to supplement petroleum based F-76 as a drop-in replacement, requiring no modifications to be done to engines currently in use. Currently, one likely candidate fuel is Hydroprocessed Renewable Diesel (HRD) derived from algae, a renewable biological source.

The first generation of Diesel biofuel is known as biodiesel. Biodiesel is produced by the transesterification of vegetable oils or animal fats into fatty acid methyl esters (FAMES) or fatty acid ethyl esters. Biodiesel and biodiesel blends have been banned from use in deployable and tactical DoD military engines due to issues with fuel storage and handling; including water entrapment, formation of fuel-water emulsions, facilitation of microbial contamination and chemical degradation [6].

HRD is a second generation biofuel. It is referred to by different names—Hydroprocessed or Hydrotreated Renewable Diesel or simply Renewable Diesel. For the purpose of this paper, it will be called Hydroprocessed Renewable Diesel or HRD. Hydroprocessed Vegetable Oils (HVO) is a broad term used to describe either HRD or Hydroprocessed Renewable Jet fuel (HRJ).

HRD is also produced from biologically-based oils, such as vegetable oils, animal fats, or oils from other plant life such as algae. However, unlike first-generation biodiesel, the hydrotreating process used to create HRD removes oxygen from the chemical makeup of the fuel resulting in a pure hydrocarbon fuel which eliminates the problems mentioned above with biodiesel. The hydrotreating process is already utilized by petroleum refineries today, simplifying production.

B. MOTIVATION

The Office of Naval Research (ONR) criteria for acceptable renewable fuels for Naval use are: “Alternative fuels aboard Navy ships must be compatible with current Navy fuels, tolerant to seawater compensation, have flash point characteristics equivalent to current Navy fuels, have long-term storage capabilities, resistance to biocontamination, and will not negatively impact the current Navy fuels logistics.” [4].

Algae HRD meets the above requirements, but knowledge of HRD combustion performance within Naval Diesel engines is not sufficient. “Research needs to address a methodology for fuel characterization and combustion qualification for acceptable operation of current and proposed gas turbines and Diesel engines that may be deployed by the Navy and Marine Corps” [4].

Most liquid fuel properties of the algae-based HRD used in this study are similar to that of F-76 with the exception of cetane number (CN). CN is often directly related to the delay before autoignition occurs in a Diesel engine, a metric known as ignition delay (IGD). IGD is the time or crank angle degree (CAD) between start of injection (SOI) and start of combustion (SOC) [7]. The CN of F-76 is 46 compared with the much higher 78 for HRD [8].

C. LITERATURE REVIEW

1. Hydroprocessed Renewable Diesel Performance

While combusting HVO in a direct injection turbocharged small automobile engine, Sugiyama et al. [9] found that HVO combustion decreased hydrocarbon emissions with reduced fuel consumption of up to 5% compared to number 2 Diesel fuel (conventional Diesel fuel). Sugiyama’s study found that the “heat release rate was advanced with shortened ignition delay to improve combustion.” Less smoke, particulate matter and ISOF emissions were also found. Sugiyama et al. concluded: “These results indicate that HVO can be adopted in direct injection Diesel engines even at various blend ratios.”

A 2007 study by Kuronen et al. [10], which compared HVO to sulfur-free Diesel performance in multiple heavy duty Diesel engines, found that emissions from engines fueled by HVO resulted in significantly lower nitric oxides (NOx), hydrocarbons (HC), and carbon monoxide (CO). Mass-based fuel consumption was found to be 1- 2% lower due to the higher Lower Heating Value (LHV) of HVO. However, the lower density of the fuel resulted in a volumetric fuel consumption which was 5-6% higher than conventional Diesel. A similar study by Aatola et al. [11] found similar results on emissions including a 35% reduction in smoke when HVO was tested in a heavy duty

Diesel engine. By optimizing the injection timing the study suggests that even better improvements in emissions can be made.

Recent work by researchers at the United States Naval Academy (USNA) looked at the combustion performance of algae-based HRD compared to that of F-76 [12]. This study was done using an indirect injected four-stroke Diesel High Mobility Multipurpose Wheeled Vehicle (HMMWV) engine. A heat release rate analysis was conducted to compare key engine metrics such as SOI, IGD, combustion duration (CD), angle of peak pressure (AOP), peak pressure (PP), indicated mean effected pressure (IMEP), brake mean effective pressure (BMEP), brake specific fuel consumption (BSFC), and carbon dioxide ($CO_{2)}$ emissions.

The HMMWV engine used by Caton et al. has a common rail injection system which allowed SOI to be determined by measuring the rapid rise in the fuel line pressure. SOI for HRD was found to be later than F-76 across the speed load map. This is illustrated in Figure 1 with engine speed on the vertical axis and the fuel-air equivalence ratio, phi, on the horizontal axis.

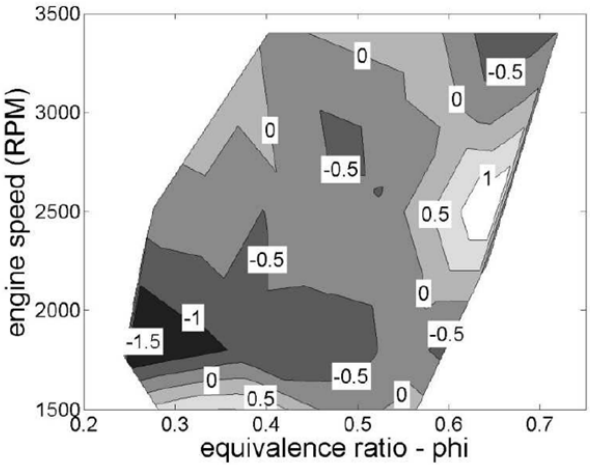

Figure 1. Start of Injection Comparison (CAD): SOI_{HRD} - SOI_D. From [12]

Ignition delay was found to be less for HRD than F-76. This study calculated IGD as the difference between SOI and 10% mass fraction burn point (CAD10). Figure 2 illustrates the difference found between the IGD of HRD to the IGD of F-76 (IGD_{HRD} –

IGD_{F76}). Negative numbers indicate that the IGD of HRD fuel was shorter than that of conventional F-76 fuel by the indicated number of CAD.

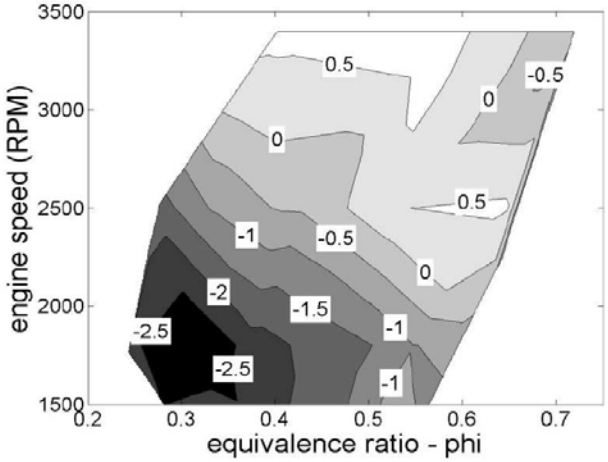

Figure 2. Ignition Delay Comparison: IGD_{HRD}-IGD_{F76}. From [12]

The study also found combustion duration (CD) to be longer for HRD by 0.5 to 1.5 CAD (Figure 3). AOP was found to be similar for HRD and Diesel (Figure 4), while PP of HRD compared to F-76 were found to be 2-6% lower (Figure5).

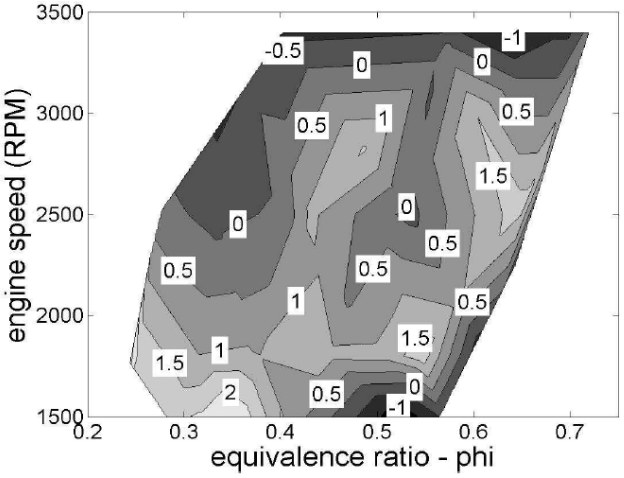

Figure 3. Combustion Duration (CAD10-CAD90) Comparison (CAD): HRD – F-76. From [12]

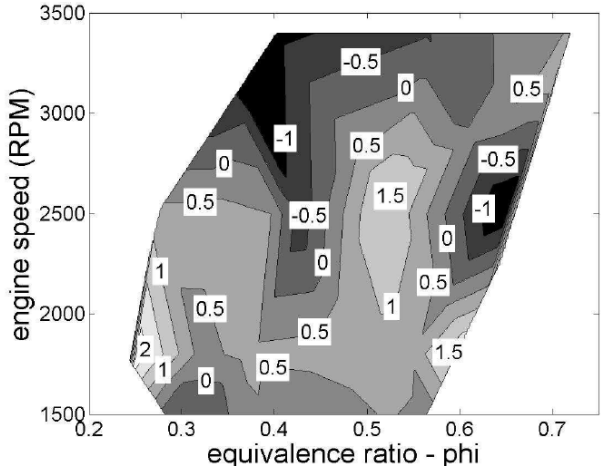

Figure 4. Angle of Peak Pressure Comparison (CAD): AOP_{HRD}-AOP_{D}. From [12]

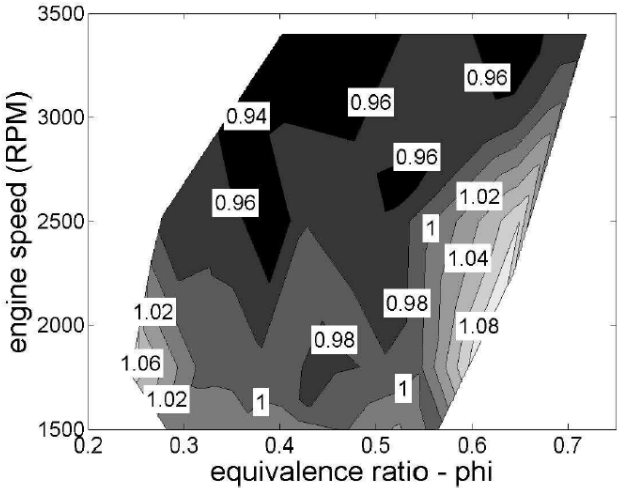

Figure 5. Peak Pressure Comparison as a Ratio: PP_{HRD}/PP_{D}. From [12]

This study concluded that the high cetane HRD fuel still maintained satisfactory engine performance overall.

2. Cetane Number Fuel Effects on Performance

Cowart et al. [14] looked at the combustion performance of multiple high CN fuels compared to that of F-76 also in a HMMWV engine. The fuels tested were hexadecane (also known as cetane), which is used as a high CN reference fuel in the ASTM cetane number test [7] with an assigned value of 100. Also investigated were a Fischer-Tropsch (FT) fuel with a high CN of 75, JP-5 with a CN of 46, and F-76 with a

CN of 44. An interesting finding from this research was that even though the FT fuel and JP-5 have a higher CN than F-76, the IGD for the two fuels was longer. The authors hypothesize that this is due to the fuels reduced density which leads to slower penetration into the combustion chamber.

To better understand the effects CN has on combustion, Olree and Lenane [13] tested fuels with CN ranging from 35 to 55. Their study compared the different fuels IGD and max rate of pressure rise (MRR). SOI was determined by the output of the injector needle-lift signal. IGD was found to correlate with CN as expected; the higher the CN the lower the IGD across the engine points tested. Olree and Lenane comment on how IGD affects the MRR within the cylinder: "Longer ignition delays contribute to an increase in premixed fuel charge that is formed during the ignition period. What appears to be a small change in ignition delay can cause a large change in the amount of premixed fuel available for uncontrolled combustion because the rate of fuel being injected increases rapidly during the delay period." Figure 6 displays the results and correlations this study found between CN and MRR.

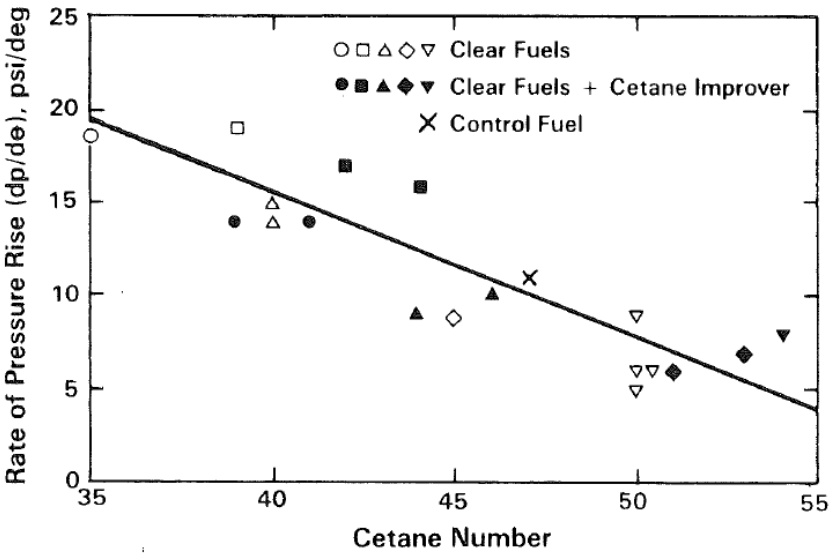

Figure 6. Max Rate of Rise vs. CN 2,000 rpm, 1/2 load, 75^{O} F inlet air. From [13]

Another study by Caton et al. compared the IGD of more than 20 simple, pure fuel components using a single cylinder Diesel engine known as a Cooperative Fuels

Research Engine (CFR) [15]. The goal of this study was to identify which fuel properties affected IGD and to find a correlation between those properties and IGD. The study concluded that a longer IGD was generally observed with decreasing liquid fuel density, kinematic viscosity, and liquid-air surface tension. Longer IGD were also observed for fuels with higher fuel volatility, as measured by boiling point and vapor pressure [15]. Figure 7 displays the correlation between CN and IGD found in this study.

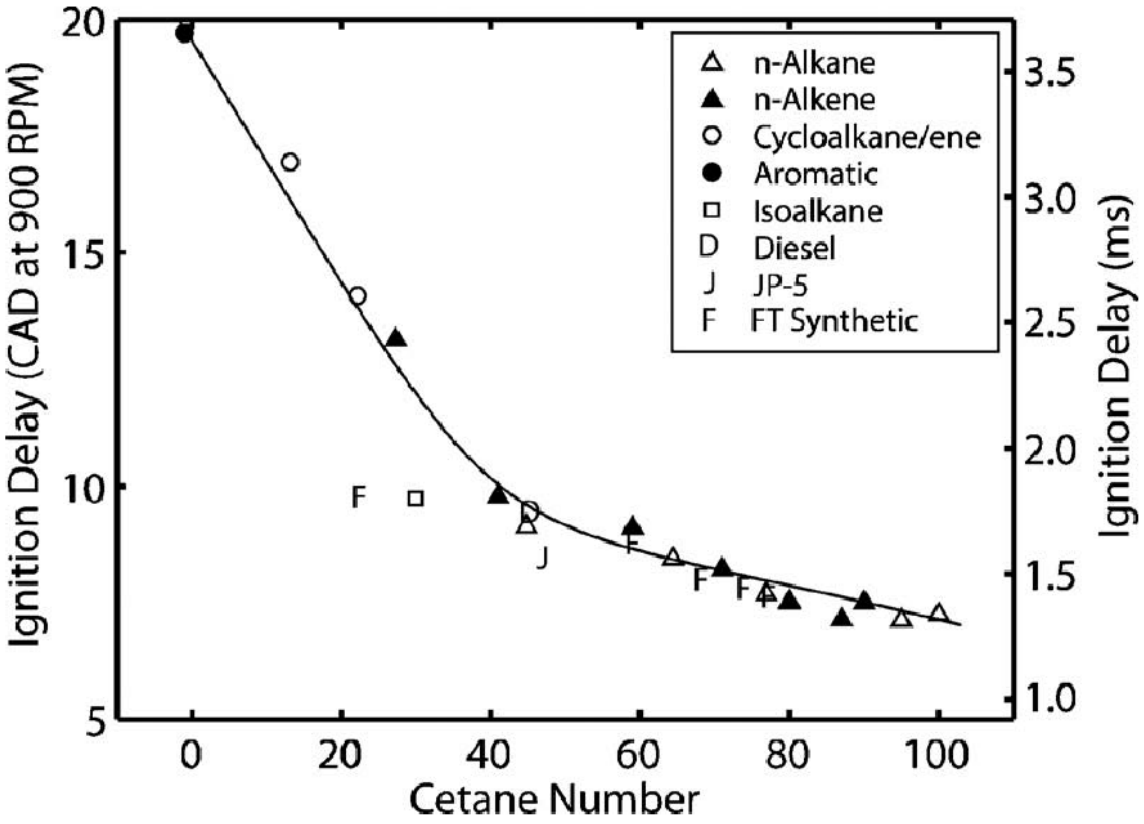

Figure 7. Ignition Delay in CAD and time (ms) of various pure component and conventional and synthetic fuel mixtures with respect to CN. From [15].

3. Determining SOI with Unit Injectors

At the University of Michigan, Filipi et al. [16] used a strain gauge mounted on the rocker arm that actuates the unit injector to determine SOI. The unit injector in this study was electronically controlled and used in a turbocharged heavy duty direct injected Diesel engine. SOI was found by first converting the strain signal to pressure then

graphed as a function of CAD. Figure 8 displays a graph of this study's results. The injection pressure was determined by the following equation, where F_{pl} is the force acting on the injector plunger and d_{pl} is the diameter of the injector plunger.

$$P_{inj} = \frac{4F_{pl}}{d_{pl}^2 \pi} \tag{1}$$

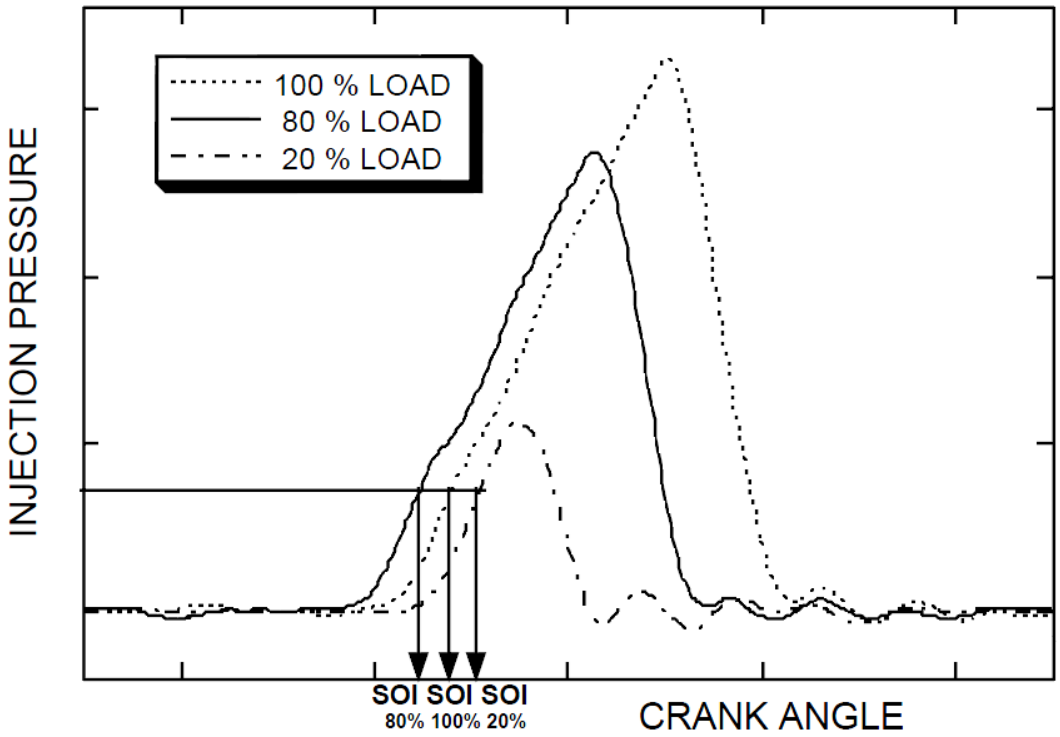

Figure 8. Injection Pressure Histories, 100%, 80% and 20% load points. From [16].

4. Summary

Based on the research above it is known that HRD used in different types of Diesel engines reduces fuel consumption and lessens NOx, HC, CO, and particulate emissions when compared to petroleum based Diesel. Multiple studies have confirmed that the higher the CN fuel used - the shorter the IGD. A MRR comparison between CN fuels spanning from 35 to 55 determined that within that CN range MRR decreases as CN increases. A thorough combustion performance analysis of HRD, investigating IGD, PP, AOP, and CD of HRD compared to conventional Diesel has been done in a four-stroke

indirect injected Diesel engine which concluded that HRD use resulted in satisfactory performance.

5. Uncertainty in Literature

A detailed combustion performance analysis including metrics such as IGD, PP, MRR, CD and CP on HRD has not been conducted using all representative Navy engines, such as a two-stroke direct injected Diesel.

D. OBJECTIVES

1. Test and Measure

Successfully operate the two-stroke direct injected Detroit Diesel test engine on algae-based HRD fuel, F-76 and blends of the two, measuring relevant combustion cycle quantities, including in-cylinder pressure, crank-angle position, and air-fuel flow rates.

2. Determine and Compare Combustion Characteristics

Reduce the acquired data across speed and load ranges of the engine to calculate and compare the following combustion characteristics of the fuels tested:

- Start of Injection
- Ignition Delay
- Max Rate of Pressure Rise
- Peak Pressure
- Angle of Peak Pressure
- Combustion Duration
- Combustion Phasing

3. Articulate Differences and Potential Problem Areas with HRD and HRD/F-76 blend use in Naval Diesel Engines.

Understand and explain differences between HRD and F-76 in order to find any areas of problematic operation when using HRD or HRD/F-76 blends as drop-in replacements. Identifying any potential benefits that could be realized in using this alternative fuel.

E. ORGANIZATION

Chapter II describes the engine and experimental setup used to obtain the combustion data.

Chapter III covers the experimental procedures.

Chapter IV discusses the heat release rate analysis and key metrics used to compare the HRD, F-76 and blends combustion performance.

Chapter V gives the experimental results and discusses the findings.

Chapter VI provides the conclusions obtained from the results.

THIS PAGE INTENTIONALLY LEFT BLANK

II. EXPERIMENTAL SETUP

A. TEST ENGINE

1. Detroit Diesel 3-53

The engine used in the study is an in-line three-cylinder, direct injected two-stroke Detroit Diesel 3-53. The engine utilizes a roots blower to boost the intake air. The engine utilizes a uniflow-scavenging configuration with intake ports around the cylinder walls and 4 exhaust valves per cylinder. Table 1 lists the key specifications and the engine is pictured in Figure 9. This engine was used to power the Army semi-amphibious vehicle, the Gamma Goat. It is representative of many Diesel engines currently in use by the Navy.

Table 1. Specifications for Detroit 3-53. From [17].

Model Number	5033-5001N
Number of Cylinders	3
Bore and Stroke	3.875 x 4.5 inches
Engine Displacement	159 cubic inches
Compression Ratio	21:1
Maximum Power Output	101 hp at 2,800 RPM
Peak Torque	205 ft-lbs at 1,560 RPM
Brake Mean Effective Pressure	97 lb/in^2

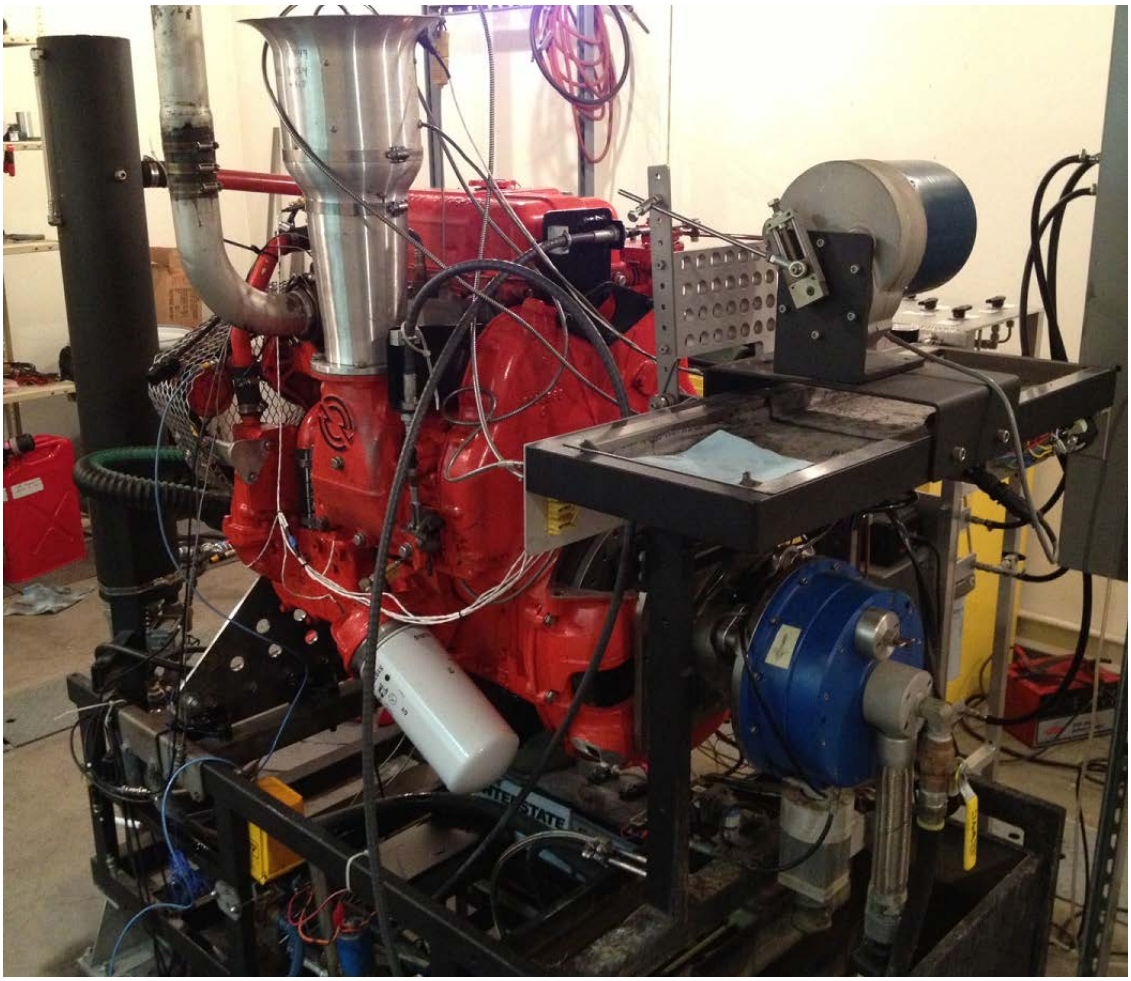

Figure 9. Test Engine: Detroit Diesel 3-53

2. Dynamometer and Engine Controls

Engine operation is controlled by a SuperFlow SF-901 system. Key components of the system include a water brake dynamometer, fuel supply system, engine cooling system and the engine control console. The engine is instrumented with oil, cooling water, and exhaust temperature sensors, a 6.5 inch diameter air intake flow meter, two fuel turbine flow meters and an oil pressure sensor. The instrument signals feed into the SuperFlow system to allow monitoring of brake performance and operating conditions. A companion computer system running SuperFlow's data acquisition software, WinDyn, is used to record the brake performance data and parameters. Figure 10 displays the SuperFlow system.

Figure 10. SuperFlow Control Console

B. FUEL SYSTEM

1. Fuel Distribution Stand

To accommodate testing of HRD and HRD blends with the existing Diesel fuel system, a fuel distribution and delivery stand was designed and built (Figure 11). The stand contains the needed valve logic, filtration and transfer pumps for selecting the requisite fuel for testing. Switching between a test fuel and Diesel was accomplished by turning the proper sequence of valves located on the top of the stand. Along with proper flushing, this system ensures no cross contamination between fuels can occur.

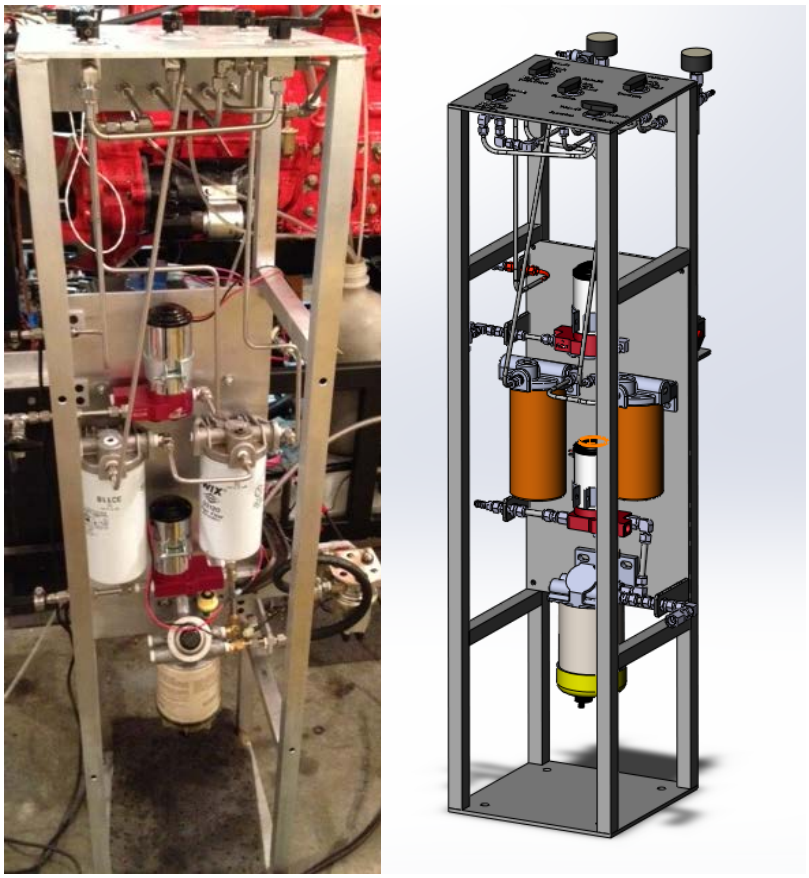

Figure 11. Fuel Distribution Stand

2. Gravimetric Fuel System

To accurately determine the specific fuel consumption and efficiency of the engine, a gravimetric fuel system was constructed (Figure 12). A flow diagram of the entire fuel system is shown in Figure 13.

The gravimetric system consists of a stainless steel basket used to hold the fuel which is attached to a Futek model LSB303 load cell. A fuel resistant rubber gasket is used to isolate the basket from its supply-and-return tubing to ensure the load cell only weighs the basket and the fuel within it. The load cell signal is sent to a data acquisition system controlled by LabVIEW. The output of the gravimetric system is displayed in LabVIEW.

Figure 12. Gravimetric System

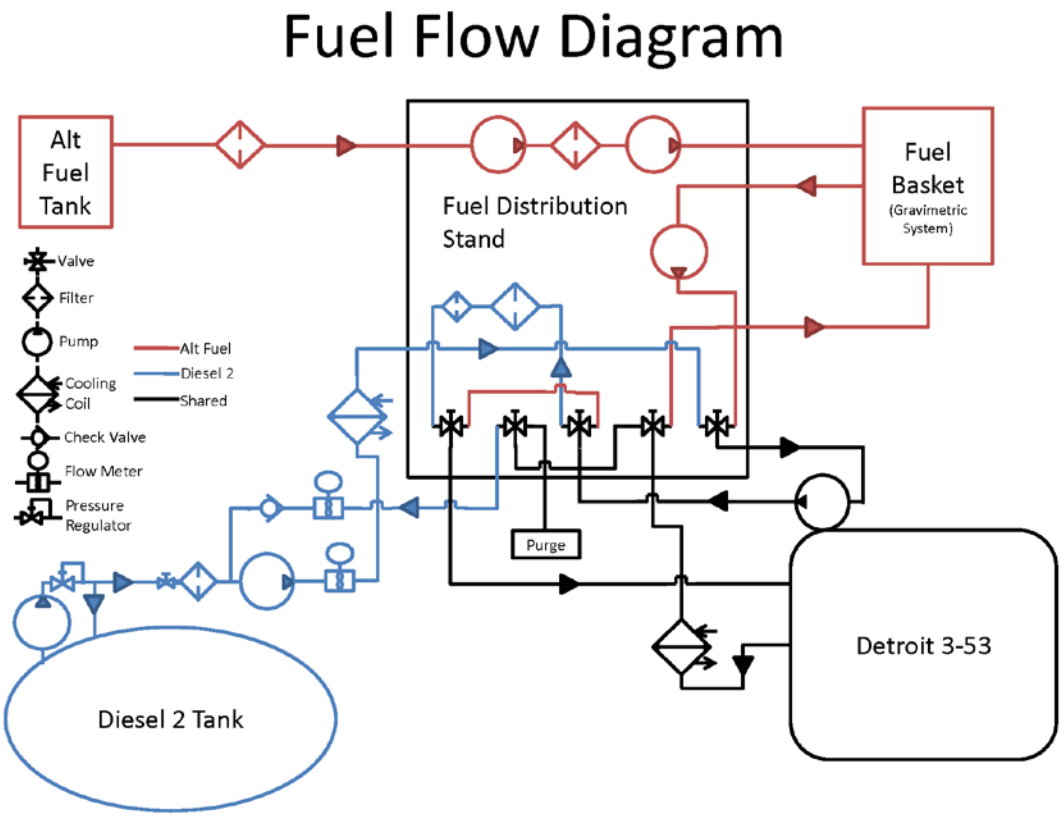

Figure 13. Fuel Flow Diagram.

C. INJECTOR ROCKER ARM STRAIN GAUGE

To characterize the SOI in the test engine a strain gauge was mounted on the rocker arm that actuates the mechanical unit injector. A Micro-Measurements strain gauge model WK-06-062TT-350 was used. The gauge was arranged in a half-bridge configuration and an instrumentation amplifier was developed to enhance the signal before it was recorded. Figure 14 shows the gauge on the rocker arm during calibration.

Figure 14. Mechanical Injector Rocker Arm Strain Gauge.

D. DATA ACQUISITION

1. Pressure Sensor and Optical Encoder

To obtain the necessary in-cylinder pressure measurements the engine has a Kistler type 6125A piezoelectric pressure sensor mounted in one of the glow plug ports. The glow plugs are unnecessary for the conditions within the engine test cell and therefore provide an ideal location for the sensor. The Kistler sensor signal is first conditioned by a Kistler dual mode 5010 charge amplifier before entering the data acquisition system.

A BEI Sensors DHM5 optical encoder with 0.5° resolution (720 pulses per revolution) is connected to the crank shaft via a flexible link. In conjunction with the

pressure sensor this allows measurement of engine crank position. Crank position is measured in degrees with top center indicated as 0° or 360°. An optical isolator module from BEI is used to isolate the encoder signals before they are acquired by the computer system. This module also reduces common-mode noise by comparison of the complementary encoder channels.

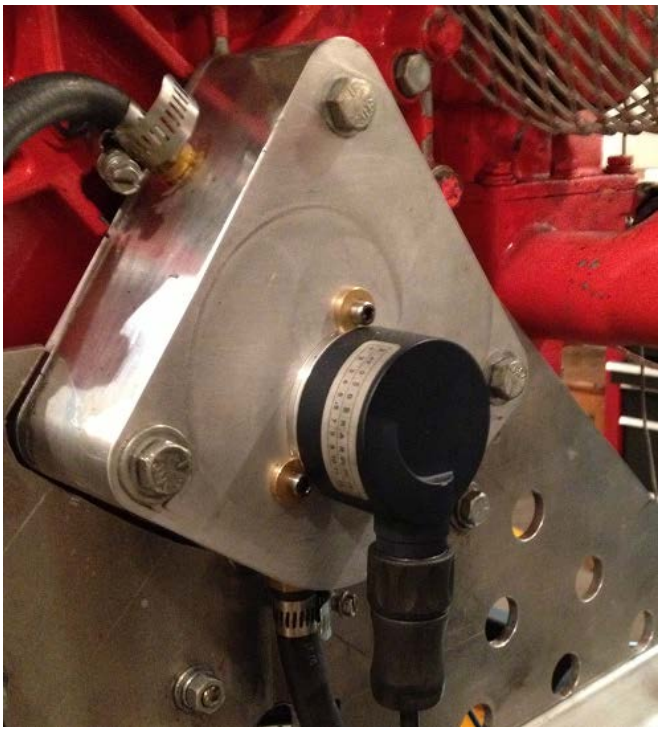

Figure 15. BEI Optical Encoder

2. Data Acquisition Systems

a. LabVIEW

A National Instruments (NI) LabVIEW based data acquisition (DAQ) was used to acquire signals from the rocker arm strain gauge, gravimetric load cell, cyclinder pressure sensor, and optical encoder. A stand-alone computer running LabVIEW 2010 software and two NI DAQ boards, NI PCI-6281 and NI PCI-6602 (counter-timer specific board), was used to acquire data from the engine system. The pressure, strain gauge and fuel weight signals are input into the NI PCI-6281 DAQ board via a NI SCB-68 connector block and the encoder signal first enters a NI BNC-2121 connecter block

before entering the NI PCI-6602 DAQ board. The LabVIEW virtual instrument (VI) records data at a rate of 50 kHz.

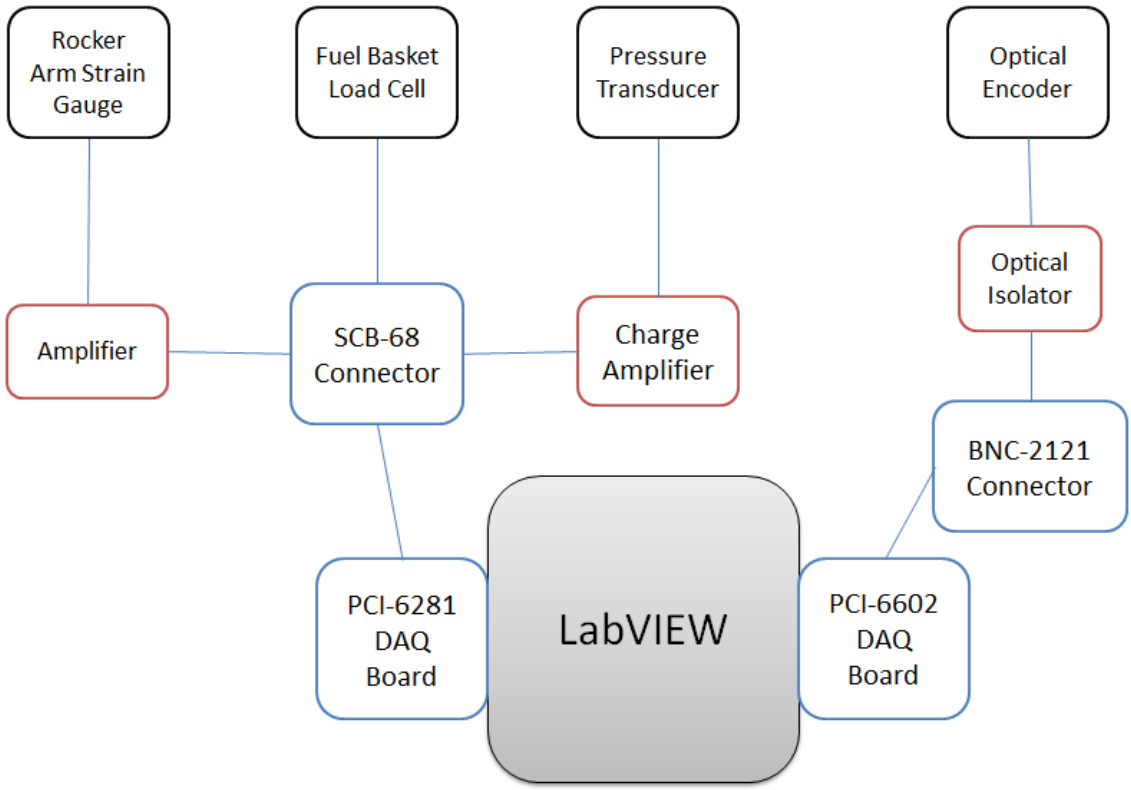

Figure 16. LabVIEW Setup

b. Hi-Techniques Synergy System

A Hi-Techniques Synergy Data Acquisition System was also used to collect the pressure and encoder data. This system is Windows 7, PC based which runs Hi-Techniques REVelation II Combustion Analysis Software. Unlike the LabVIEW system, which acquires data on a time basis, the Synergy System is triggered to record the pressure signal by the encoder or every 0.5 CAD or 720 pulses per revolution. Figure 17 depicts the Synergy setup.

Figure 17. Synergy System Setup. From [18].

E. FUELS TESTED

Algae HRD and F-76 were provided to NPS by Naval Air Systems Command (NAVAIR). Operation of neat (100%) Algae HRD and F-76 was compared along with 25/75, 50/50, and 75/25 blends of HRD/F76, respectively. Combustion performance was compared to that of neat F-76. The fuel blends were volumetrically mixed on the day of testing. The HRD tested meets or exceeds most standards for F-76 listed in MIL-DTL-16884L [19]. The density of HRD is 0.781 kg/L which is lower than the minimum standard of 0.8 kg/L. The CN of HRD is higher than the upper limit of 67. Tables 2 and 3 provide a summary of the relevant properties of the fuels tested. Table 2 lists ONR fuel data on HRD and F-76. Table 3 has cetane numbers of HRD/F-76 blends obtained from testing by Southwest Research Institute (SwRI).

The fuel was blended volumetrically using two liter (L) graduated cylinders with 10 milliliter (mL) accuracy. Prior to testing 12 L of each fuel blend was mixed, sufficient for all tests so remixing was not required. After the proper amounts of HRD and F-76 were measured, they were mixed in a five-gallon bucket. The bucket was thoroughly shaken to ensure proper blending.[1]

[1] Confirmed by SwRI Senior Research Scientist, Becky Nelson, to be an acceptable fuel blending technique [20]

Table 2. Fuel Data. From [8].

Test	Method	Units	Min	Max	HRD	50/50 HRD/F-76	Petroleum F-76 used in Blend
Density at 15°C	D4052	kg/L	0.800	0.876	0.781	0.813	0.845
Cetane Number, Derived	ASTM D6890	--	42	67	78	63	46
Cloud Point	D5773	°C		-1	-5	-12.2	-13.6
Hydrogen Content	D7171	Mass %	12.5		14.7	13.8	12.9
Heating Value	D4809	MJ/kg	43.0		44.1	43.3	42.6

Table 3. Cetane Number of HRD/F-76 Blends. From [21]

Test	Method	25/75 HRD/F-76	50/50 HRD/F-76	75/25 HRD/F-76
Cetane Number	D613	56	66	72

III. TESTING PROCEDURES

A. TEST MATRIX

A test matrix of 10 speed load points was developed to represent the full operating range of the engine. All fuels were tested on the same day at the same operating points. Before testing the engine was warmed up to normal operating conditions using conventional Diesel from the main fuel tank at MPL. The order of testing is represented in Table 4 by the numbers within the matrix. The temperature, humidity and pressure of the engine test cell were recorded for each speed load point for each fuel tested. A standard operating procedure (SOP) was developed to ensure the accuracy and that all the necessary data was recorded. The testing SOP can be seen in Appendix B.

Table 4. Test matrix, engine speed and load. Numbers in matrix represent test order.

Fuel Testing Matrix					
Torque [ft-lbs]	Engine Speed [rpm]				
		550	1,100	1,650	2,200
	50	1	2	5	
	100		3	6	9
	150		4	7	10
	190			8	

B. FUEL FLUSHING

When switching between fuels, care was taken to ensure the fuel system had been completely flushed. A detailed flushing procedure was developed and followed to ensure no fuel cross contamination. A copy of the procedure is in Appendix A. The SOP

provides instructions for changing fuels used within the basket or if switching to a test fuel after using conventional Diesel from the main tank. In short, a sufficient quantity of the next fuel to be tested was pumped through the systems components to purge the fuel remaining from the previous test. That flushing fuel was then drained from the fuel basket and the test fuel was pumped in.

C. FUEL CONSUMPTION

The signal from the load cell attached to the fuel basket was calibrated to weight in pounds (lbs). To obtain more accurate fuel consumption values, a LabVIEW script was developed to fit a line to weight data recorded over 90 seconds using a least squares approach. The slope of the line represents the fuel consumption of the engine in lbs/sec.

D. IN-CYLINDER PRESSURE COLLECTION

The Synergy and LabVIEW systems were used simultaneously to collect the pressure and CAD data for each speed load point tested. The Synergy system collected 100 cycles at 0.5° resolution and LabVIEW collected data at a rate of 50 kHz for 4 seconds. At 550 rpm LabVIEW was able to record 5,450 samples per revolution for 36 complete cycles. At 2,200 rpm LabVIEW collected 1,360 samples per revolution for 146 complete cycles. Internally, the LabVIEW model linearly interpolates between encoder counts (0.500°) to output CAD data discretized every 0.125°. The assumption behind this interpolation is that engine crankshaft speed varies insignificantly over the 0.5° region between encoder pulses. This interpolation allows much finer resolution of combustion metric timing such as start-of-combustion and ignition delay.

IV. ANALYSIS

A. HEAT RELEASE RATE ANALYSIS

1. Overview

A Heat Release Rate Analysis of the engine cycle data allows for the rate of energy released by the fuel within the engine to be determined during each increment of CAD. The total energy of the system consists of the work done on the piston, the increase of internal energy of the air-fuel mixture and the heat transferred though the cylinder walls [22]. This analysis allows for important metrics like combustion phasing, combustion duration, and SOC to be determined. When combustion changes from the premixed to the diffusion flame can also be determined from this analysis.

The theory for the heat release analysis used in this thesis was adapted from official course notes from the internal combustion engines class at the US Naval Academy [23].

2. Control Mass Energy Analysis

While the engine ports and valves are closed it is assumed no mass escapes the system (blowby gases are ignored). Equation 3 represents the total energy change in the closed system.

$$dU = -pdV - \delta Q_H \tag{3}$$

where U equals the internal energy, p represents the pressure within the cylinder, V is the volume of the combustion chamber at any instant and the Q_H is the energy lost through the cylinder walls by heat transfer. This equation represents a first-law energy balance in which changes in internal energy are balanced by transfers of work or heat out of the control mass system.

The internal energy of the fuel air mixture can be separated into its chemical and sensible heat parts. Knowing the change in sensible internal energy for ideal gases:

$$\delta Q_{sensible} = m c_v dT \ , \tag{4}$$

where m is mass, c_v is specific heat at a constant volume and T is the temperature of the gas, and the change in chemical energy of the fuel-air mixture is represented by δQ_{ch}, dU becomes:

$$dU = m c_v \, dT + \delta Q_{ch} \tag{5}$$

As the energy in the fuel is released, $\frac{\delta Q_{ch}}{dt}$, is negative so the signs become positive on the right hand side of Equation 3. Substituting Equation 5 into Equation 3 and dividing by dt yields:

$$\frac{\delta Q_{ch}}{dt} = p\frac{dV}{dt} + m c_v \frac{dT}{dt} + \frac{\delta Q_H}{dt} \tag{6}$$

Equation 6 shows that the rate of change in chemical energy of the fuel-air mixture (energy in the fuel) equals the rate of work done on the piston plus the rate of change of sensible energy within the cylinder plus the rate of heat transfer. Figure 18 is a pictorial representation of this.

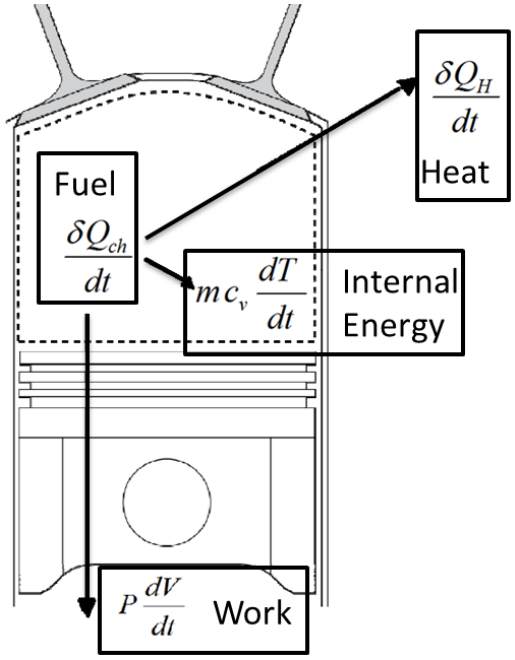

Figure 18. Heat Release Diagram. Modified from [23]

To solve Equation 6, first differentiate the ideal gas law and solve for dT, treating mR_{spec} as a constant:

$$pV = mR_{spec}T \tag{7}$$

$$Vdp + pdV = mR_{spec} \times dT \tag{8}$$

$$dT = \frac{1}{mR_{spec}}(Vdp + pdV) \tag{9}$$

From the definition of enthalpy and the ratio of specific heats:

$$\frac{R_{spec}}{c_v} = k - 1 \tag{10}$$

Substituting Equation 9 and 10 into Equation 6 yields:

$$\frac{\delta Q_{ch}}{dt} = \frac{k}{k-1} p \frac{dV}{dt} + \frac{1}{k-1} V \frac{dp}{dt} + \frac{\delta Q_H}{dt} \tag{11}$$

Equation 11 was used to determine the heat release rate for this thesis. From the pressure and volume data p, V, $\frac{dp}{dt}$, and $\frac{dV}{dt}$ are known. The ratio of specific heats for the combustion chamber gases and the heat transfer term still needs to be determined.

3. Determining *k* for the Combustion Gases

The value of k varies with temperature and therefore the combustion gas temperature, T_{CG}, is required. To calculate T_{CG}, the ideal gas law is utilized.

$$T_{CG} = \frac{pV}{mR_{spec}} \tag{12}$$

To find the mass of the combustion gases in the cylinder to solve Equation 12, the timing of when the intake ports and exhaust valves are closed is needed. For cylinder one this was determined to be between -90 CAD and 90 CAD from the event timing bar graph (Figure 19). During this portion of the cycle the mass is assumed to be constant.

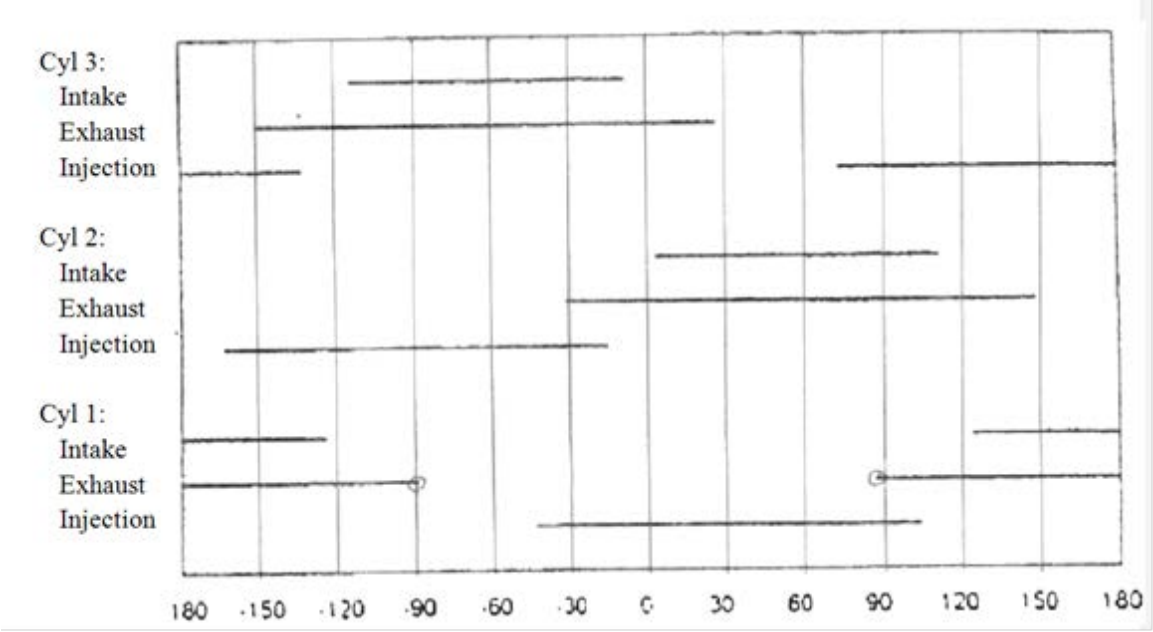

Figure 19. Detroit Diesel 3-53 Engine Event Timing

By assuming the temperature of the air during the gas exchange process is 350 K, knowing the pressure of the intake air measured from the manifold and by calculating the volume of the combustion chamber at -90 CAD, the ideal gas law can be used to solve for the mass of the combustion gases. Now that the mass is known, T_{CG} can be solved for.

4. Determining the Heat Transfer Term

The heat transfer to the surroundings of the engine is assumed to be all due to convection and solved using Equation 13, the convective heat transfer equation:

$$\delta Q_H = h_C A(T_{CG} - T_W) \tag{13}$$

The instantaneous surface area, *A*, of the combustion chamber is solved knowing the engine geometry and the CAD. The temperature of the combustion chamber walls, T_W, was assumed to be constant at 400 K.

The convective heat transfer coefficient, h_c, was estimated using Woschni's correlation, referenced in Heywood [24].

$$h_c\left(W/m^2 \cdot K\right) = 3.26B(m)^{-0.2}\, p(kPa)^{0.8} T(K)^{-0.55} w(m/s)^{0.8} \tag{14}$$

In the above correlation; B is the cylinder bore, the pressure, p is the instantaneous cylinder pressure and T equals T_{CG}. The w above represents the average cylinder gas velocity and is defined by the following:

$$w = \left[C_1 \bar{S}_p + C_2 \frac{V_d T_r}{P_r V_r} (P - P_m) \right] \tag{15}$$

where $\bar{S}_p$ is the average piston speed in *m/s*, V_d is the cylinder displaced volume in m^3, T_r (*K*), P_r (*kPa*), and V_r (m^3) are of the combustion chamber gases at a reference state. In this thesis, the reference state was chosen at the location of exhaust valve closing at -90 CAD. In Equation 15, P_m (*kPa*) is the motored cylinder pressure at the same CAD as P (*kPa*). The constants for Equation 13 are defined below:

For the gas exchange period (90 CAD to -90 CAD): C_1=6.18, C_2=0

For the compression period (-90 CAD to SOC): C_1=2.28, C_2=0

For the combustion period (SOC – 90CAD): C_1=2.28, C_2=3.24×10^{-3}

5. Heat Transfer Coefficient Scaling

The heat transfer coefficient found using Woschni's correlation provides an accurate profile of the heat transfer throughout an engine's cycle however it needs to be scaled for use with a specific engine and for different speed-load conditions. In order to determine an accurate scaling coefficient, the fuel energy for one cycle is compared to the predicted total energy release determined by the cumulative heat release rate. Assuming complete combustion, the total energy release should match the incoming fuel energy. This assumption is valid when the engine is operating normally- not sputtering or emitting black smoke, clear indicators that the all of the fuel has not burned.

The energy in fuel per revolution (FCR), is determined from the fuel consumption (FC) data found by the gravimetric system:

$$FC(lbs/s) \times \frac{1}{2.205}(kg/lbs) \times 60(s/\min) \times \frac{1}{EngRPM}(\min/rev) = FCR(kg/rev) \tag{16}$$

Next the lower heating value (LHV) of the fuel is used to determine the energy per cycle:

$$FCR(kg/rev)\times LHV(MJ/kg)\times\frac{1}{3}(cylinders)\times 1\times 10^{6}(J/MJ)=FE\,\frac{J}{rev} \qquad (17)$$

The heat transfer coefficient is then scaled so the cumulative energy release is equivalent to the energy in the fuel.

B. COMBUSTION METRICS ANALYSIS

Using the principles outlined in the explanation of the heat release analysis, the above analysis was conducted by post-processing raw engine data using a code based in MATLAB. First, text files of the pressure data were read into MATLAB and the multiple revolutions collected for the speed-load points were each individually analyzed for all the relevant combustion metrics. Metrics for each cycle were then averaged together to determine a mean metric value for that operating point.

To accurately compare the different combustion performance metrics in MATLAB mathematical methods needed to be created to consistently determine the metrics such as SOC. To determine SOC, first the max slope of the heat release rate was found. Then a linear projection was made from the max slope point and the intersection with zero (baseline) heat release was used to indicate SOC. Figure 20 is a pictorial representation of hoe SOC is determined.

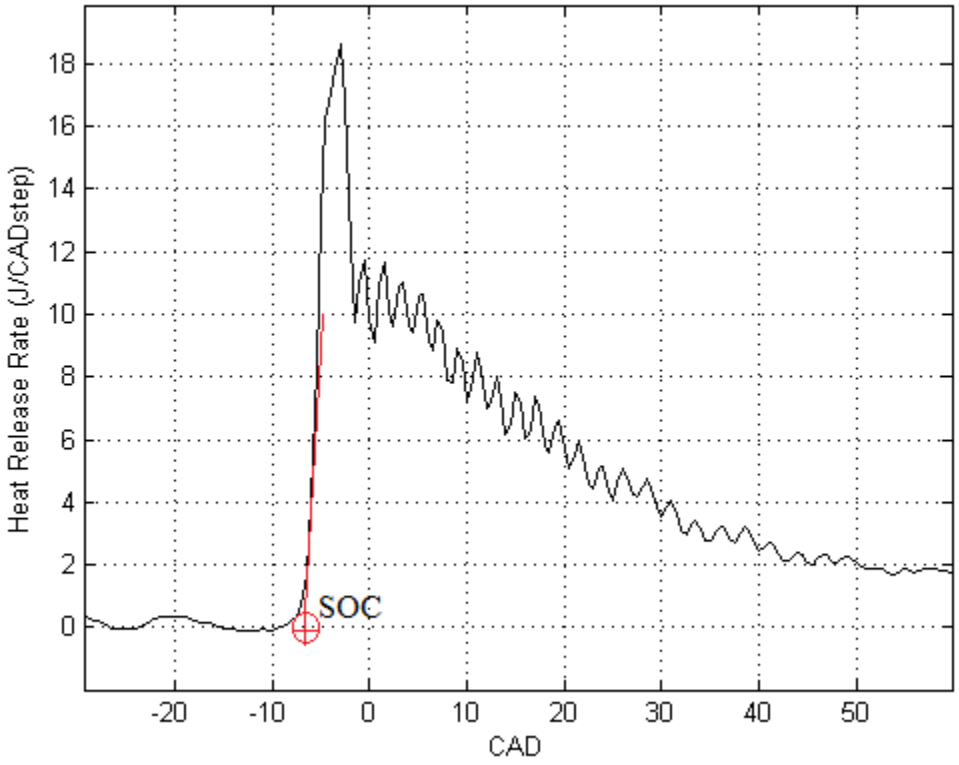

Figure 20. Determining Start of Combustion

Combustion duration (CD) for this thesis was defined as the CAD from when 10% of the fuel was consumed to when 90% of the fuel was consumed (CAD90-CAD10). CAD10 and CAD90 are determined using the cumulative sum of the heat release rate. Combustion phasing (CP) is defined as the corresponding CAD where 50% of the fuel is consumed (CAD50). CAD50 was also calculated from the cumulative sum of the heat release rate. Figure 21 displays CAD10, CAD50 and CAD90 on a cumulative heat release curve.

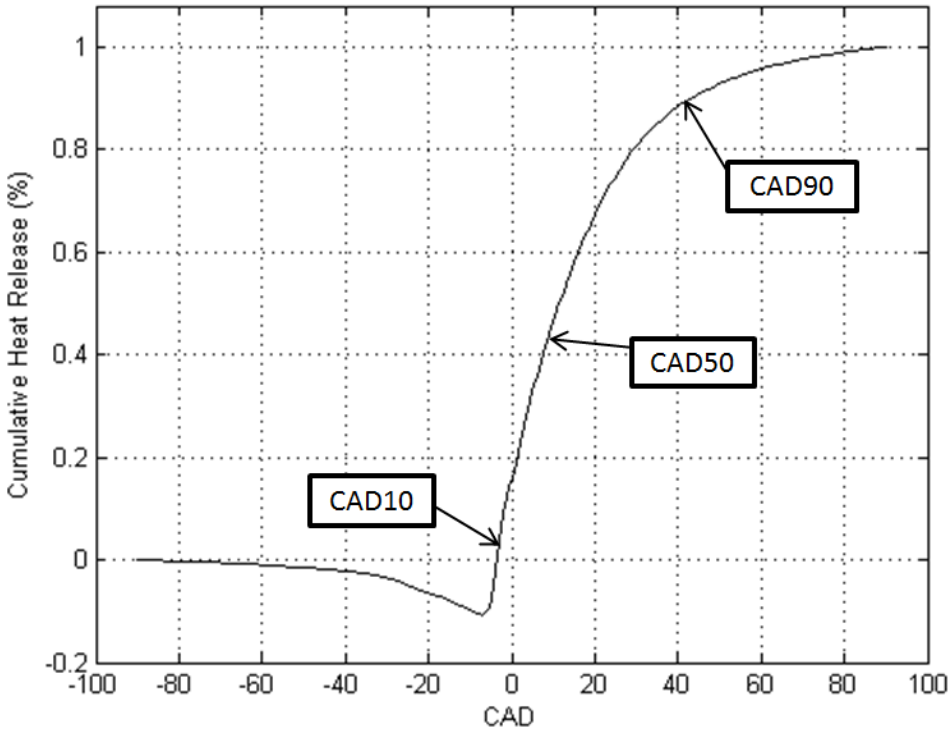

Figure 21. Determining CAD10, CAD50 and CAD90

MRR, PP, and AOP were all determined from the pressure trace. MRR is the maximum slope of the pressure trace in bar/CAD. PP is the maximum pressure and AOP is the CAD corresponding to the PP.

V. RESULTS AND DISSCUSSION

A. CHARACTERIZING START OF INJECTION

Because CN is the most conspicuous difference between HRD and F-76, measuring the IGD differences between the tested fuels and blends is a primary goal of this work. Because IGD is the difference between SOC and SOI, both must first be determined. Before this investigation it was not known how SOI, for the test engine, changed with engine speed, load or most importantly for this paper; with varying fuel types like HRD and F-76. Therefore, strain gage signals from the rocker arm were analyzed to compare how speed, load and fuel type affected the apparent SOI.

Figure 22 shows the strain gauge signal traces at 1,650 rpm and 50, 100, 150 and 190 ft-lbs of torque all for the same fuel, F-76. The signal shows an increase in strain just before TC and reaches max strain soon after. This trace looks very similar to what was shown in Figure 8 from Filipi et al. [16], including the trend in magnitudes with increasing load.

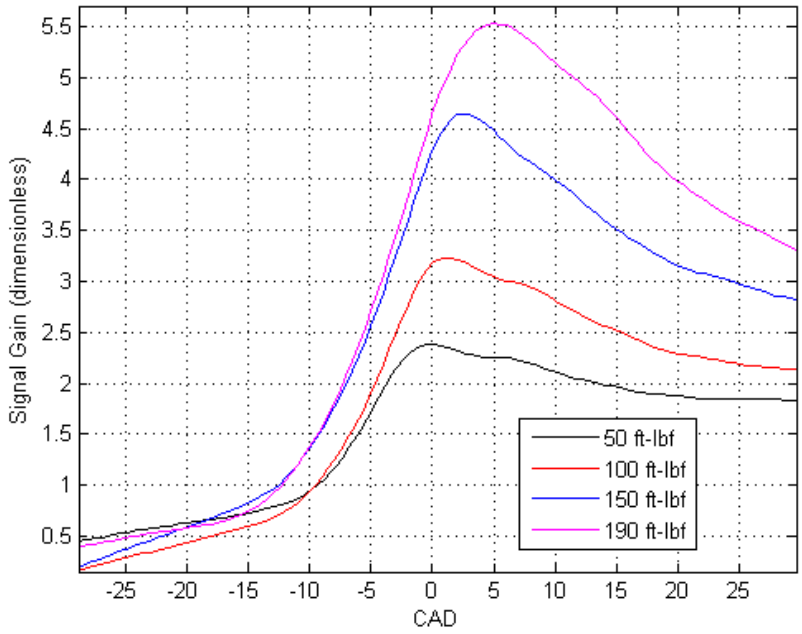

Figure 22. Raw Strain Gauge Signal, F-76 at 1,650 rpm Different Loads

The exact SOI point cannot be determined unambiguously without in situ confirmation of SOI (e.g. from an optical window). However, SOI occurs nominally at 10 CAD BTC, and qualitative trends with speed, load, and fuel type can be determined from the strain gauge data. The signal was plagued by vertical drift and some noise, so in order to compare strain traces when one variable was changed, the signal needed to be vertically shifted. They were shifted to best horizontally align the initial increase of strain common to all traces. If the signals then overlapped each other SOI was taken to have occurred at the same time. If a signal was to the left of the of the reference trace, SOI advanced and if it was to the right SOI was later. This method is not suited for determining the exact difference in SOI between traces, but it is certainly sufficient to determine qualitative characteristics.

Figure 23 shows as load was increased for a constant speed of 1,650 rpm, SOI advanced. This trend was consistent for other engine speeds.

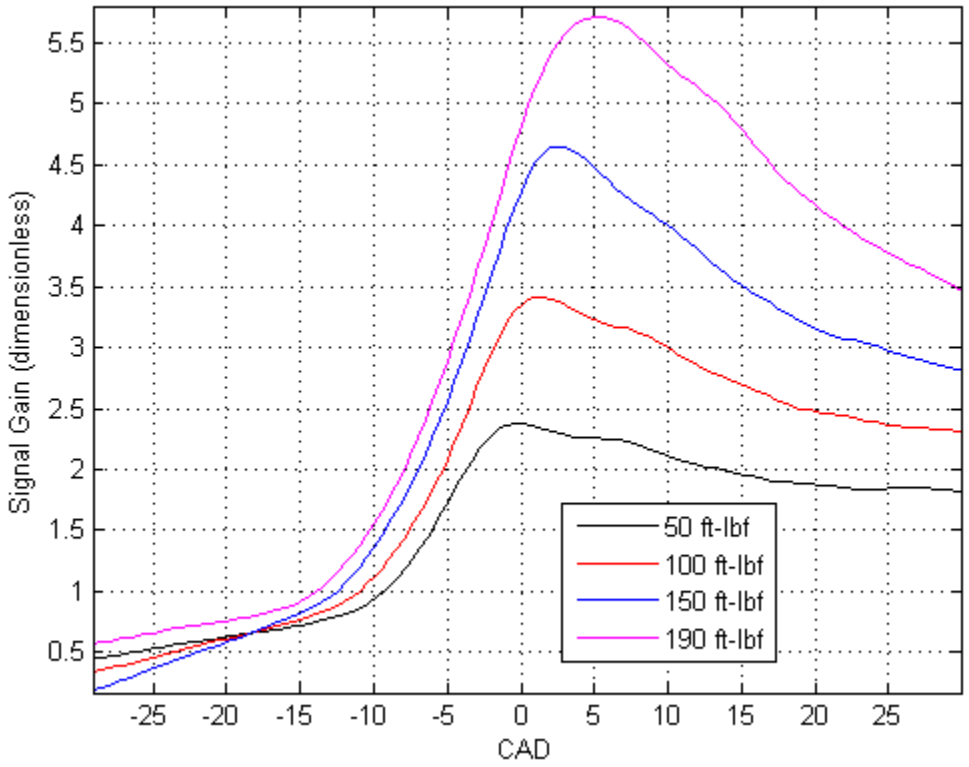

Figure 23. Aligned Strain Gauge Signal, F-76 at 1,650 rpm Different Loads

Figure 24 is a plot of the injector rocker arm strain where the load was held constant at 50 ft-lbs and the speed was varied. Figure 21 shows that as speed is increased SOI is retarded. This trend is consistent for 100 and 150 ft-lbs.

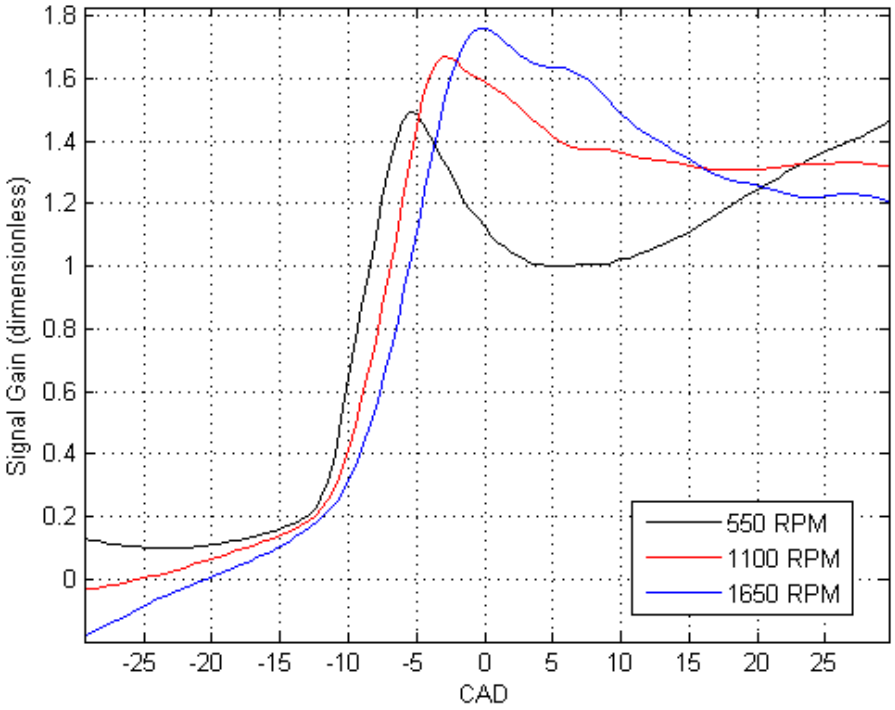

Figure 24. Strain Gauge Signal, F-76 at 50 ft-lbs Different Speeds

Figure 25 is a plot of the strain signal from neat F-76, HRD, and the three blends for 1,650 rpm and 150 ft-lbs. It shows that the SOI is insensitive to fuel change because all the traces fall on top of one another. This result is very important. Even though the SOI cannot yet be determined explicitly, we know for this engine, SOI occurs at the same CAD for F-76, HRD and blends of the two at the same speed load points. This allows comparison of relative differences in IGD between F-76 and HRD at the same speed-load points.

$$IGD = SOC - SOI \quad (18)$$

$$\Delta IGD = IGD_1 - IGD_2 = (SOC - SOI)_1 - (SOC - SOI)_2 \quad (19)$$

Subscripts 1 and 2 indicate different fuel types but at the same speed-load point. Since SOI is the same for IGD_1 and IGD_2 Equation 19 reduces to:

$$\Delta IGD = SOC_1 - SOC_2 \quad (20)$$

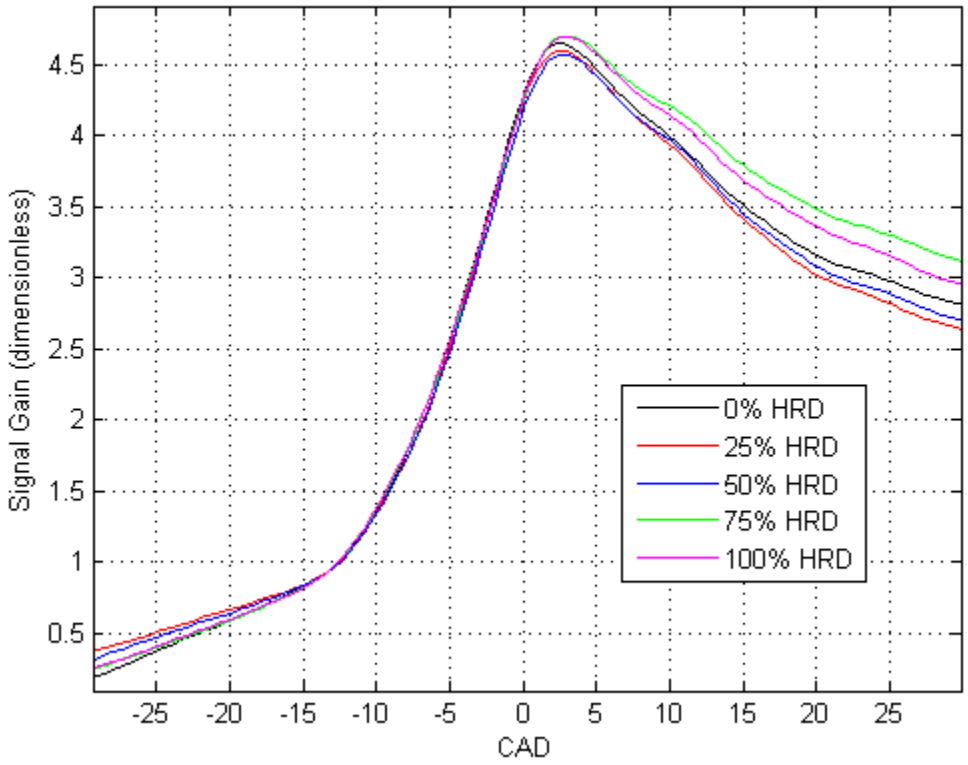

Figure 25. Strain Gauge Signal, All Fuels at 1,650 rpm 150 ft-lbs

B. PRESSURE VS. CRANK ANGLE

Figure 26 shows a pressure trace of F-76 at a moderate speed and load point. The pressure in the cylinder closely follows an isentropic compression curve until SOC. The approximate locations where the exhaust valves open (EVO) and close (EVC), as well as where the intake ports open (IPO) and close (IPC) along with SOC are labeled on Figure 23.

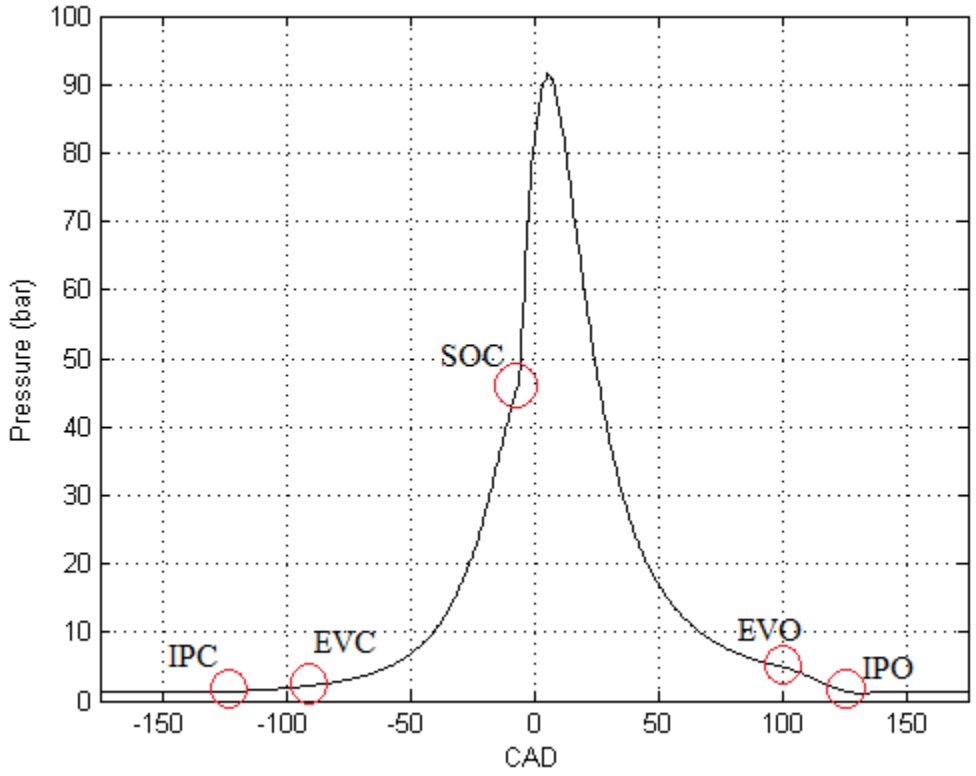

Figure 26. Pressure Trace, F-76 at 1,650 rpm 150 ft-lbs

Figure 27 shows pressure traces of F-76 at 1,650 rpm at different loads. It shows the higher pressures needed to produce higher torque. Figure 28 is an enlarged view of Figure 27 and more clearly shows the differences in SOC and peak pressures for the different loads. The following traces are ensemble averages of multiple cycles

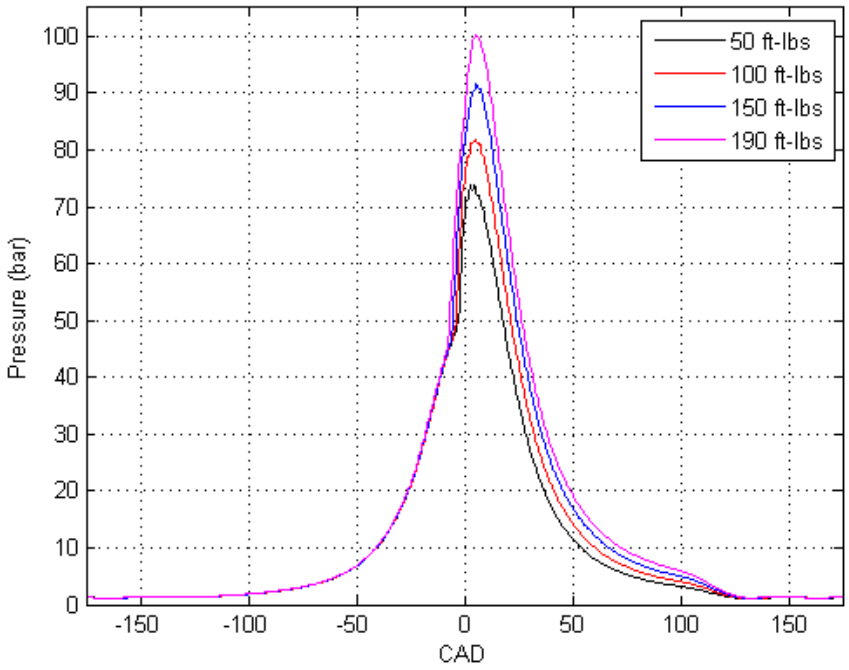

Figure 27. Pressure Trace, F-76 at 1,650 rpm and Different Loads

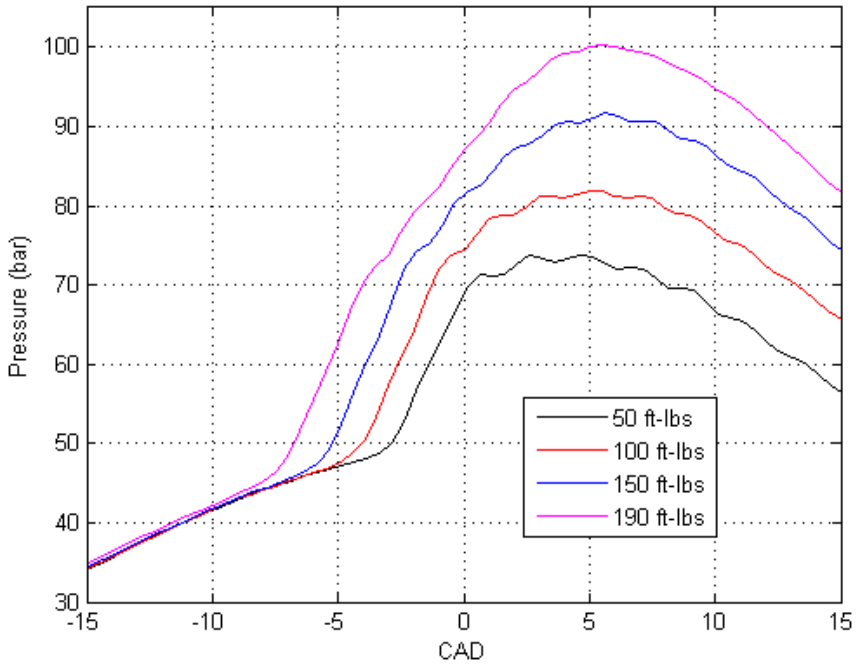

Figure 28. Pressure Trace, F-76 at 1,650 rpm and Different Loads

The pressure traces of F-76 and HRD at the same speed and load are shown in Figure 29. From this trace initial interpretations can be made for SOC, MRR, PP, and CD differences between the two fuels. HRD has an earlier SOC, a lower MRR, a lower PP and longer CD.

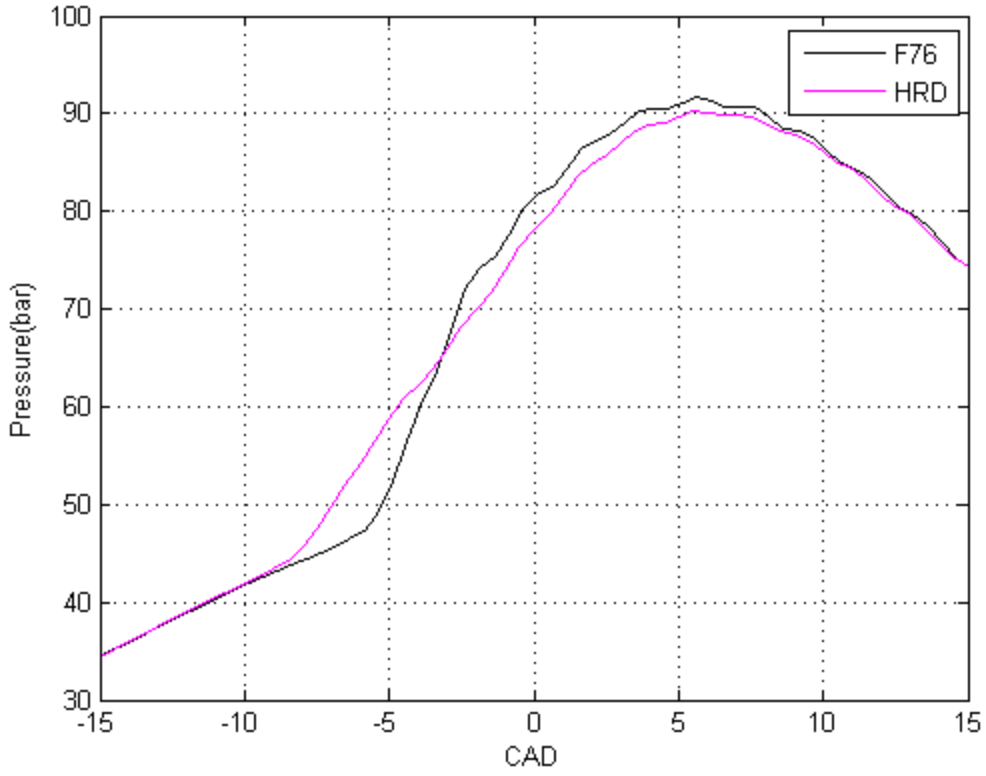

Figure 29. Pressure Traces, HRD and F-76 at 1,650 rpm 150 ft-lbs

C. HEAT RELEASE

Figure 30 shows the heat release rate of HRD and F-76 for 1,650 rpm and 150 ft-lbs. Several important differences are evident. Heat release rate from HRD starts earlier and its maximum is much lower suggesting that SOC is earlier. Advanced SOC implies a shorter IGD, as expected based on CN differences. Due to the lower rate of heat release, a lower rate of pressure rise is also expected. On the figure, the point where the premixed combustion in the cylinder ends and the controlled diffusion flame combustion begins, is marked. The premixed combustion phase of HRD ends earlier but starts sooner when compared to F-76.

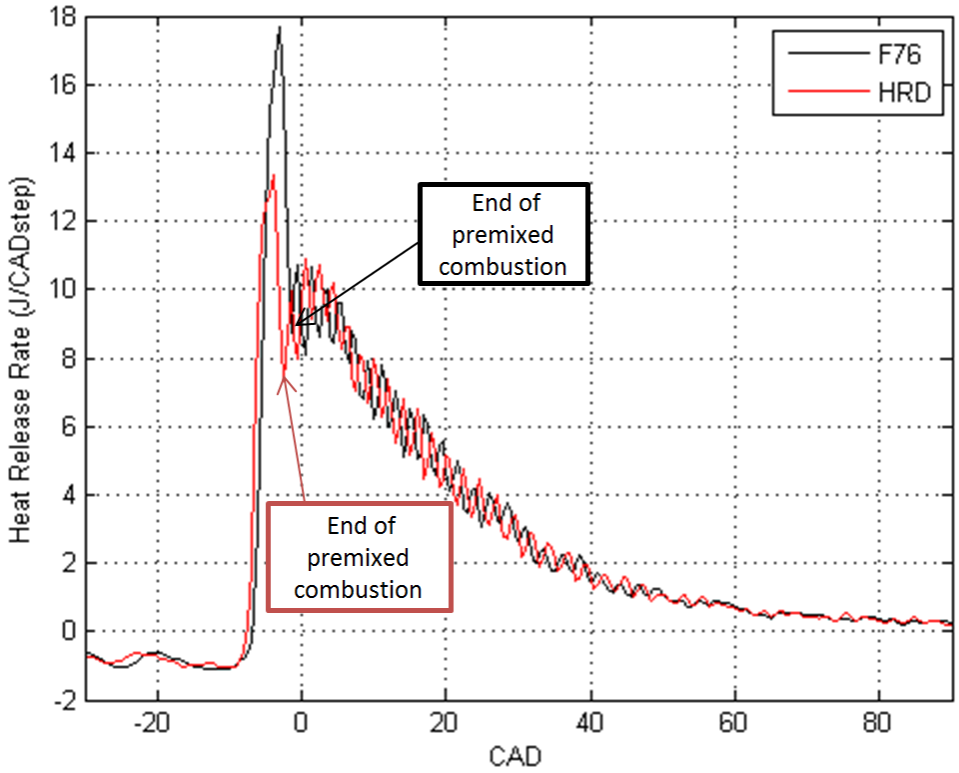

Figure 30. Heat Release Rate, HRD and F-76 at 1,650 rpm 150 ft-lbs

The cumulative heat release curves for HRD and F-76 at 1,650 rpm and 150 ft-lbs are shown in Figure 31, which are simply integrals of the heat release rate.

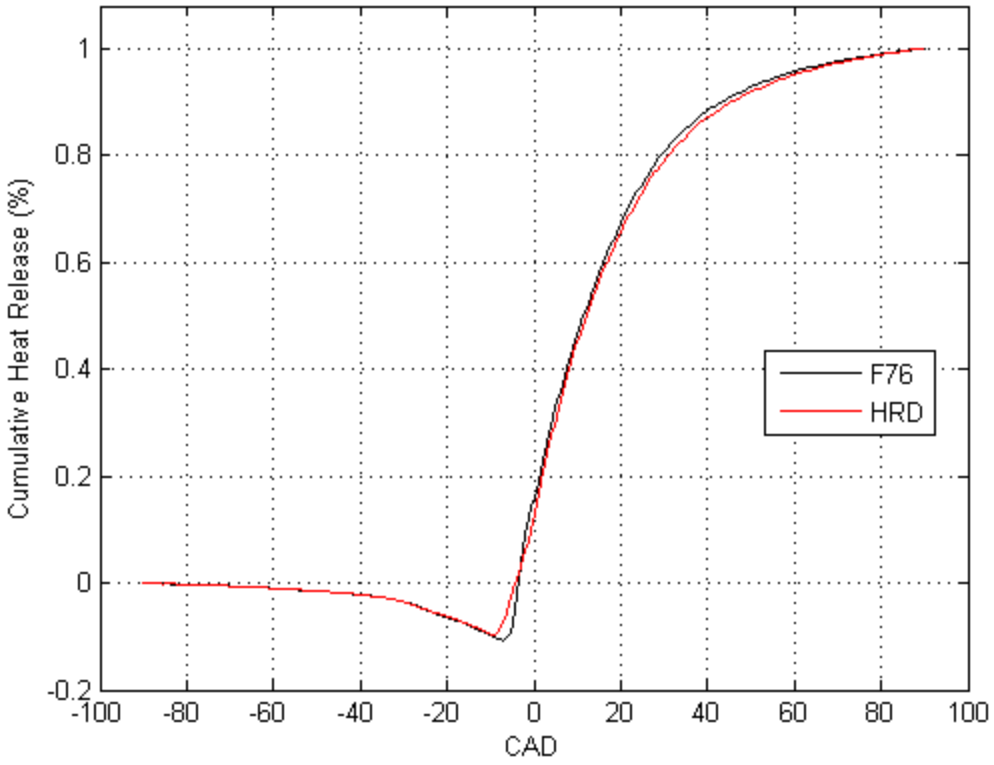

Figure 31. Cumulative Heat Release, HRD and F-76 at 1,650 rpm 150 ft-lbs

D. IGNITION DELAY

Table 5 lists the IGD difference between neat HRD and F-76 in CAD and milliseconds (ms) for all the operating points. Figure 32 graphically displays IGD differences in CAD on a contour plot and Figure 33 shows the IGD differences based on time.

Table 5. Ignition Delay Difference (CAD [ms]): IGD_{HRD}-IGD_{F76}

		Load ft-lbs			
Speed rpm		**50**	**100**	**150**	**190**
	550	-1.60 [-0.48]	X	X	X
	1,100	-2.07 [-0.31]	-2.13 [-0.32]	-1.87 [-0.28]	X
	1,650	-2.47 [-0.25]	-2.50 [-0.25]	-2.51 [-0.25]	-2.48 [-0.25]
	2,200	X	-2.48 [-0.19]	-2.43 [-0.18]	X

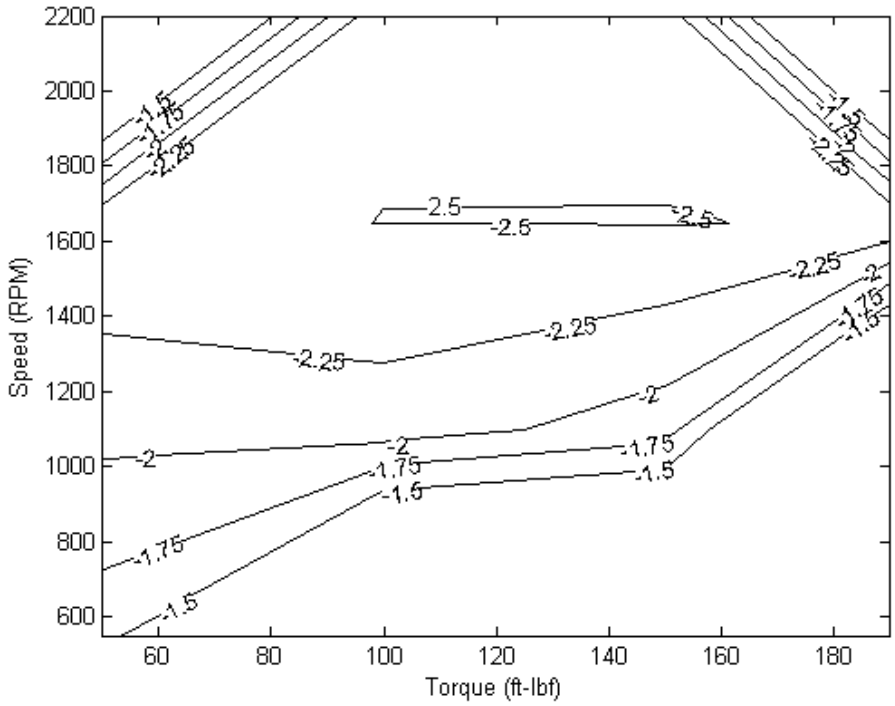

Figure 32. Ignition Delay Difference (CAD): IGD_{HRD}-IGD_{F76}

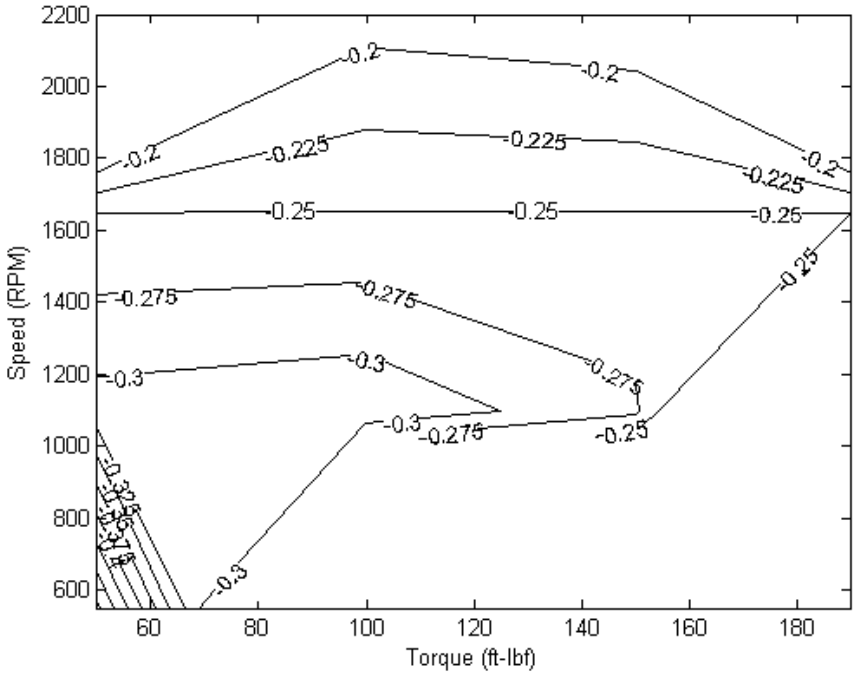

Figure 33. Ignition Delay Difference (ms): IGD_{HRD}-IGD_{F76}

Ignition delay decreased as percent HRD in the fuel increased, which directly corresponds to the increased CN of the fuel. Figure 34 is a plot of the difference between HRD and blends with F-76 at 1,650 rpm and different loads. The figure shows the strong relationship between the change in IGD as percent HRD increases. A 2.5 CAD change in IGD was the maximum which was found for engine speeds of 1,650 and 2,200 rpm at all loads. The minimum change in IGD was observed at 550 rpm and 50 ft-lbs. Based on time the difference in IGD varied from 0.48 to 0.18 ms.

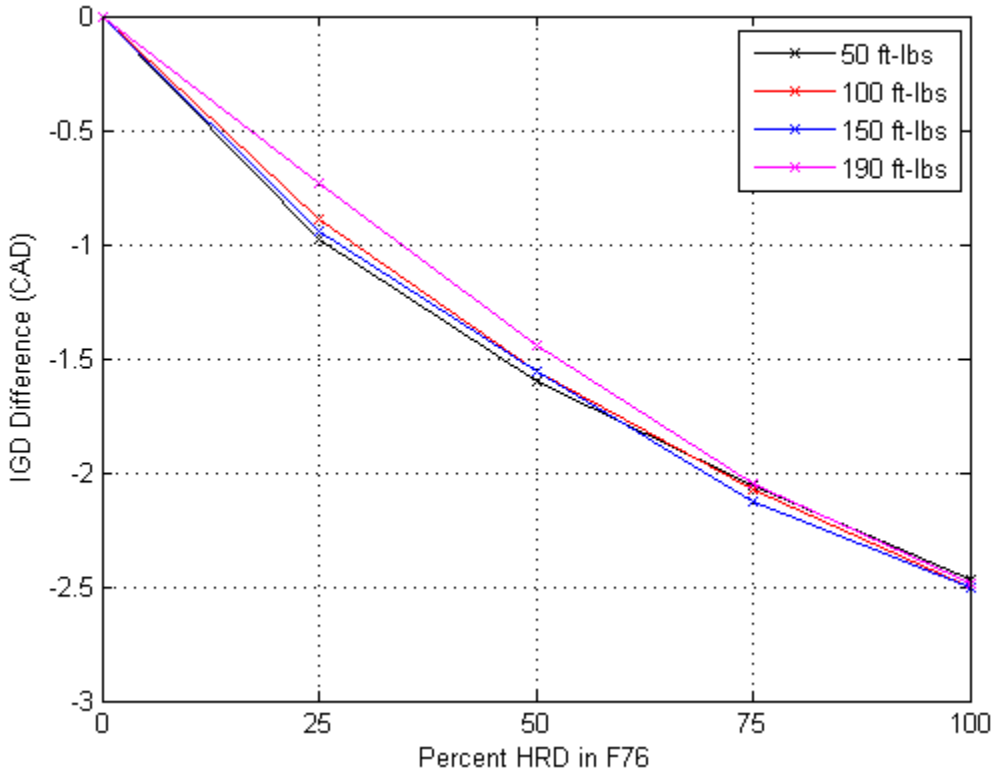

Figure 34. Ignition Delay Difference at 1,650 rpm and Different Loads: $IGD_{\%HRD}$-IGD_{F76}

E. MAX RATE OF PRESSURE RISE

Max rate of pressure rise is an important metric which represents the dynamic stress on the piston and cylinder experience due to combustion. More stress on the engine can lead to parts failing and decreased reliability. Also, MRR is related to engine noise, which is important for both commercial and military applications. The higher CN

HRD and HRD blends resulted in lower MRR. The shorter IGD results in less fuel-air premixing at SOC, which in turn results in a smaller initial premixed burn leading to a slower rate of pressure rise in the cylinder [13].

Table 6 lists the differences of MRR at each speed load point. Figure 35 displays these differences on a contour plot. Figure 36 shows the MRR for the different fuels at 1,650 rpm and different loads. Max rate of rise was substantially lower for HRD across the speed load map. The maximum difference was a 4.5 bar/CAD decrease at 1,650 rpm and 150 ft-lbs. This was a 55% reduction. The minimum change was 1.8 bar/CAD or 32% less at 1,650 rpm and 50 ft-lbs.

Table 6. Max Rate of Pressure Rise Difference (bar/CAD): MMR_{HRD}-MMR_{F76}

		Load ft-lbs			
Speed rpm		**50**	**100**	**150**	**190**
	550	-3.58			
	1,100	-4.37	-4.53	-2.99	
	1,650	-1.77	-3.98	-4.54	-2.88
	2,200		-2.18	-2.08	

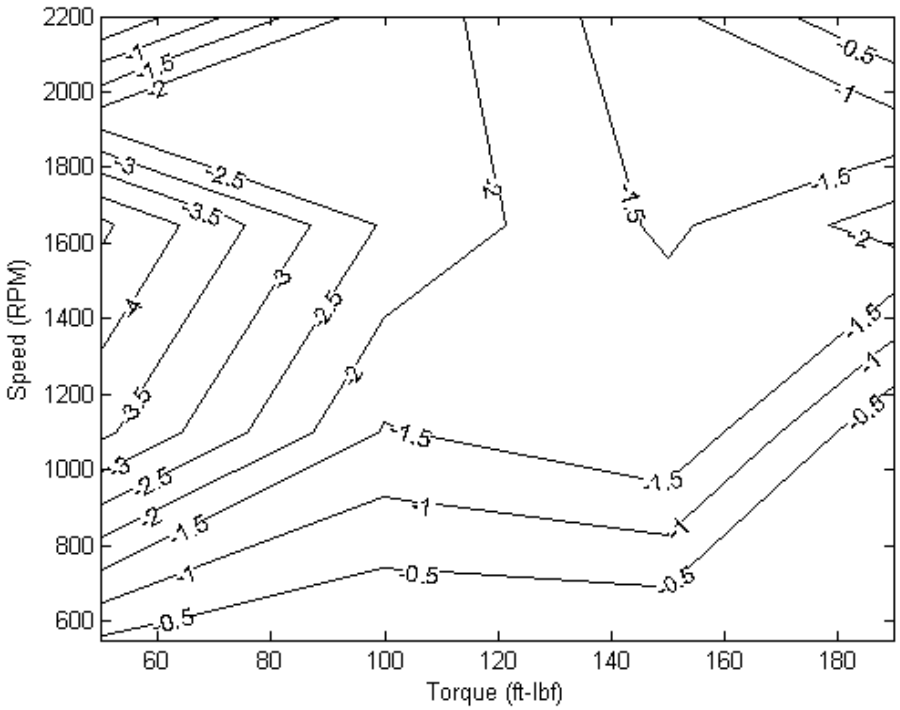

Figure 35. Max Rate of Rise Difference (bar/CAD): MRR_{HRD}-MRR_{F76}

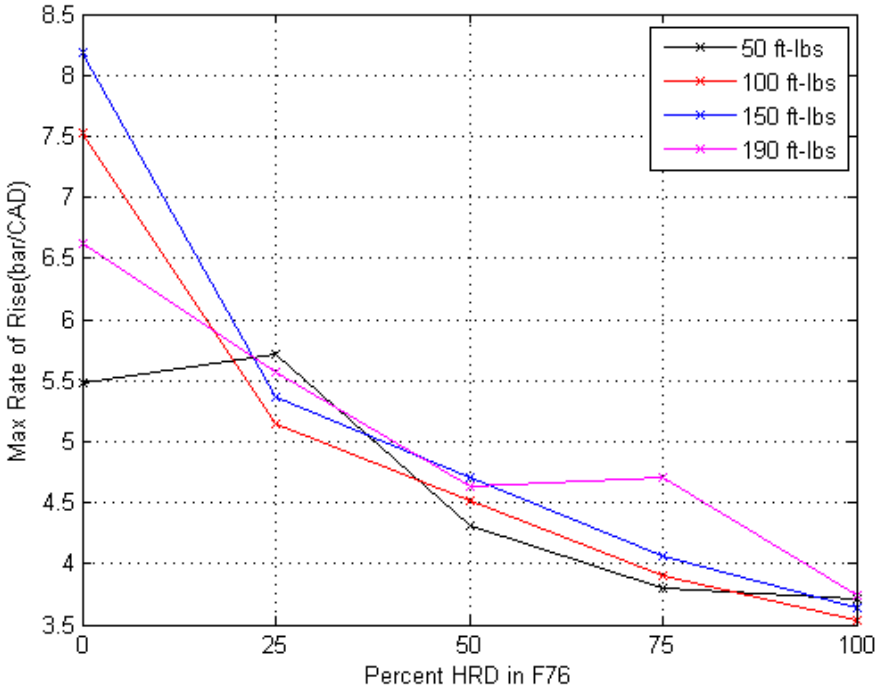

Figure 36. Max Rate of Rise, All Fuels at 1,650 rpm and Different Loads

F. PEAK PRESSURE

Peak pressure is a measure of max stress due to combustion on the piston and cylinder. Like MRR the higher stresses caused by higher PP can affect long term reliability. Peak pressure decreased across the speed load map for HRD compared to F-76. Table 7 lists these differences. Figure 37 is a contour plot of the Table 7 data and Figure 35 shows the trend of decreasing PP as percent HRD is increased for different loads at 1,650 rpm. The values of peak pressures at 1,650 rpm for all the fuels is also displayed in Figure 38. The max decrease in PP of 4.6 bar or 6% occurred at 1,650 rpm and 50 ft-lbs. The minimum difference was 0.45 bar or 0.6% lower at 550 rpm and 50 ft-lbs.

Table 7. Peak Pressure Difference (bar): PP_{HRD}-PP_{F76}

		Load ft-lbs			
Speed rpm		**50**	**100**	**150**	**190**
	550	-0.45			
	1,100	-3.60	-1.46	-1.98	
	1,650	-4.59	-2.44	-1.41	-2.24
	2,200		-2.33	-1.13	

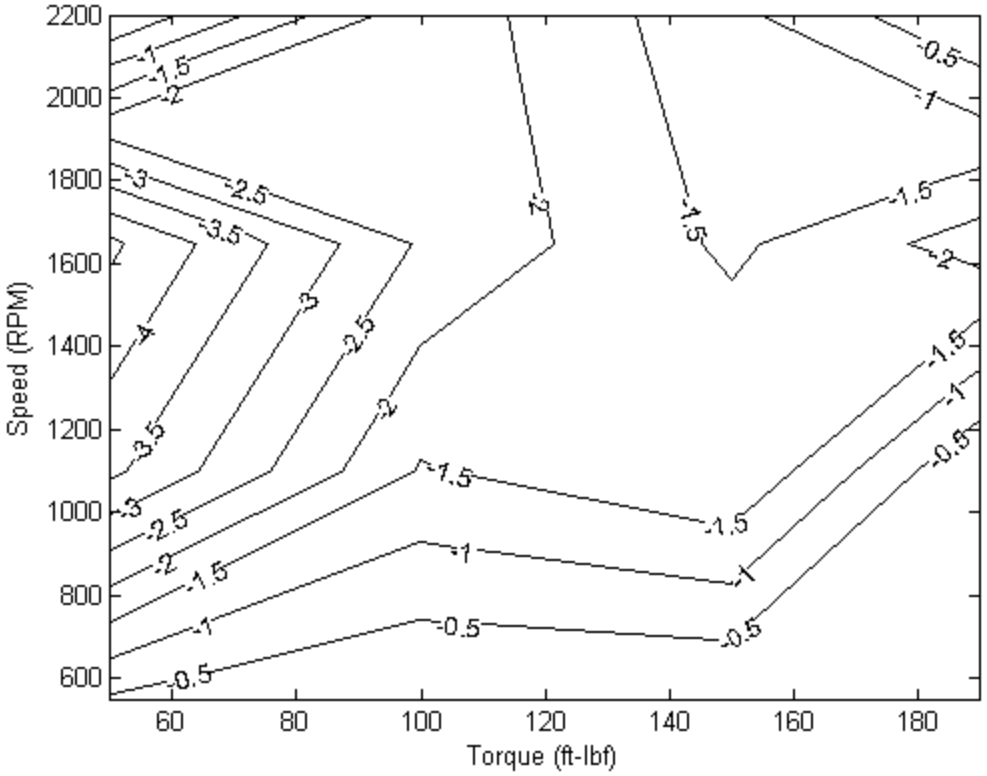

Figure 37. Peak Pressure Difference (bar): PP_{HRD}-PP_{F76}

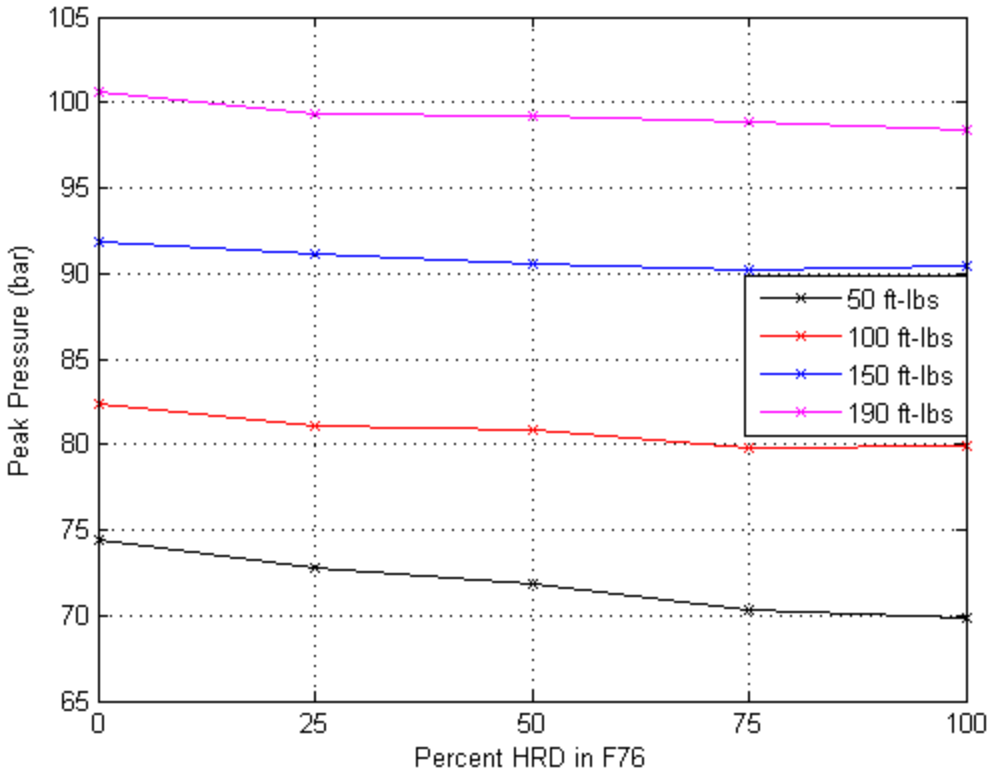

Figure 38. Peak Pressure, All Fuels at 1,650 rpm and Different Loads

G. ANGLE OF PEAK PRESSURE

There was not much of a difference between AOP of HRD and F-76. However, AOP of HRD did retard slightly. Table 8 shows that AOP was later for all operating point but one. The greatest AOP difference of 0.9 CAD occurred at 1,100 rpm 50 ft-lbs. AOP advanced at 1,650 rpm 150 ft-lbs. Figure 39 is a contour plot of the Table 8 and Figure 40 displays AOP for all fuels at 1,650 rpm and different loads.

Table 8. Angle of Peak Difference (CAD): AOP_{HRD}-AOP_{F76}

		Load ft-lbs			
Speed rpm		50	100	150	190
	550	0.06			
	1,100	0.86	0.47	0.01	
	1,650	0.88	0.29	-0.03	0.23
	2,200		0.79	0.29	

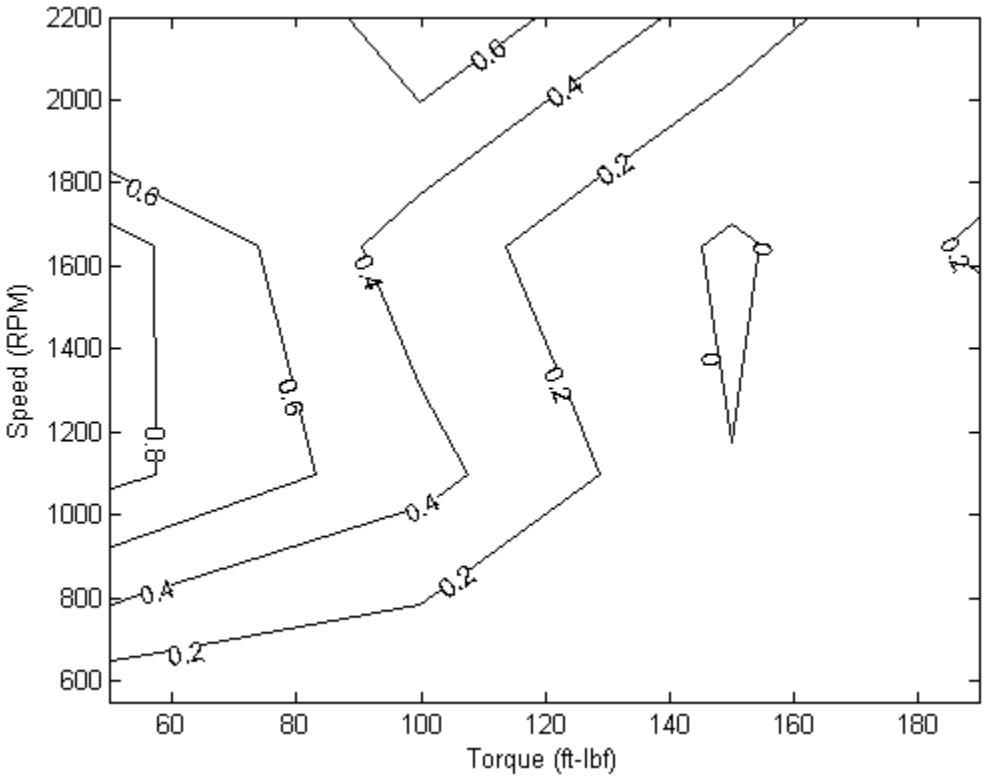

Figure 39. Angle of Peak Difference (CAD): AOP_{HRD}-AOP_{F76}

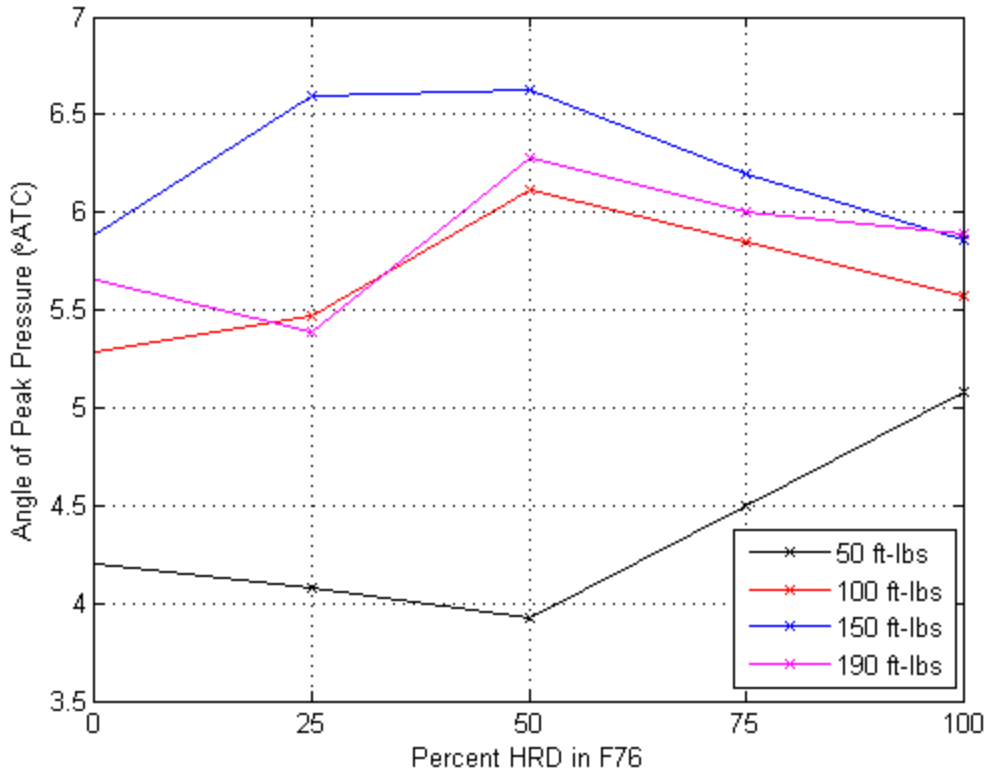

Figure 40. Angle of Peak, All Fuels at 1,650 rpm and Different Loads

H. COMBUSTION DURATION

The CD difference of HRD and F-76 is shown in Table 9 and in the contour plot of Figure 41. CD of HRD increased across the speed load map. An earlier SOC meant less premixed fuel and air when combustion began which caused a slower heat release rate all leading to a CD increase. Since the CD is longer the average pressure within the cylinder does not need to be as high to obtain the same output from the engine. The maximum change in CD of 3.2 CAD or an 8% increase occurred at 1,650 rpm and 50 ft-lbs. The minimum change in CD of 0.7 CAD or a 2% increase occurred at 550 rpm and 50 ft-lbs. Figure 42 shows the increase in CD as %HRD increases for different loads at 1,650 rpm.

Table 9. Combustion Duration Difference (CAD): $(CAD90\text{-}CAD10)_{HRD}$-$(CAD90\text{-}CAD10)_{F76}$

		Load ft-lbs			
		50	**100**	**150**	**190**
Speed rpm	**550**	0.69			
	1,100	2.91	2.26	2.32	
	1,650	3.16	2.33	2.79	1.90
	2,200		2.24	1.85	

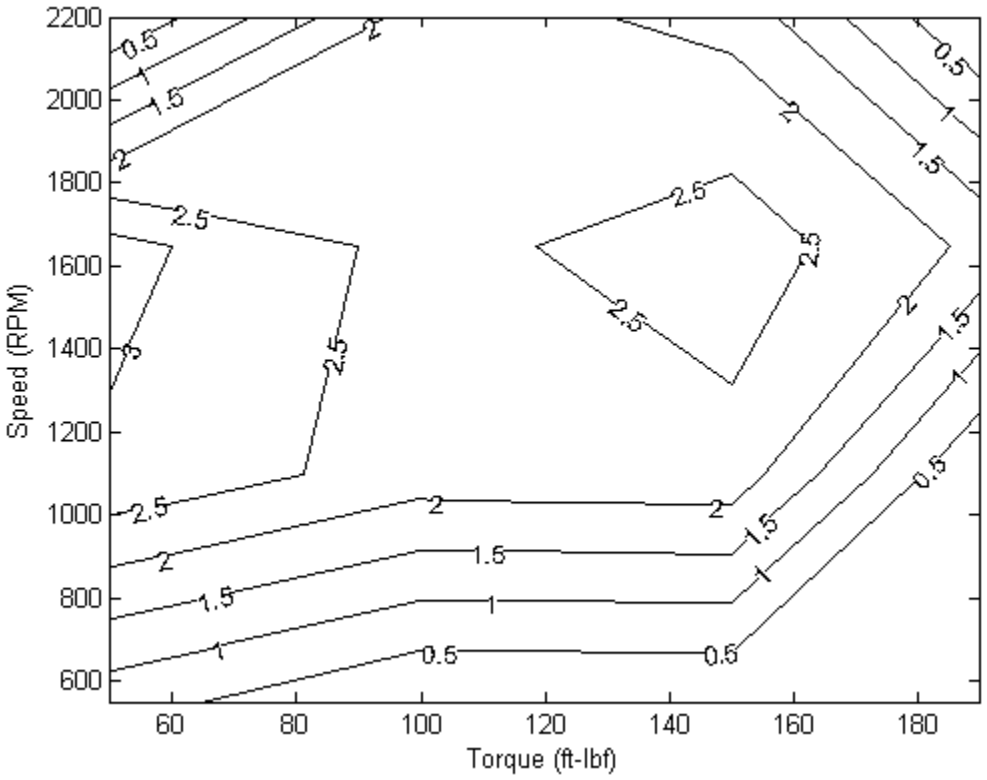

Figure 41. Combustion Duration Difference(CAD): $(CAD90\text{-}CAD10)_{HRD}$-$(CAD90\text{-}CAD10)_{F76}$

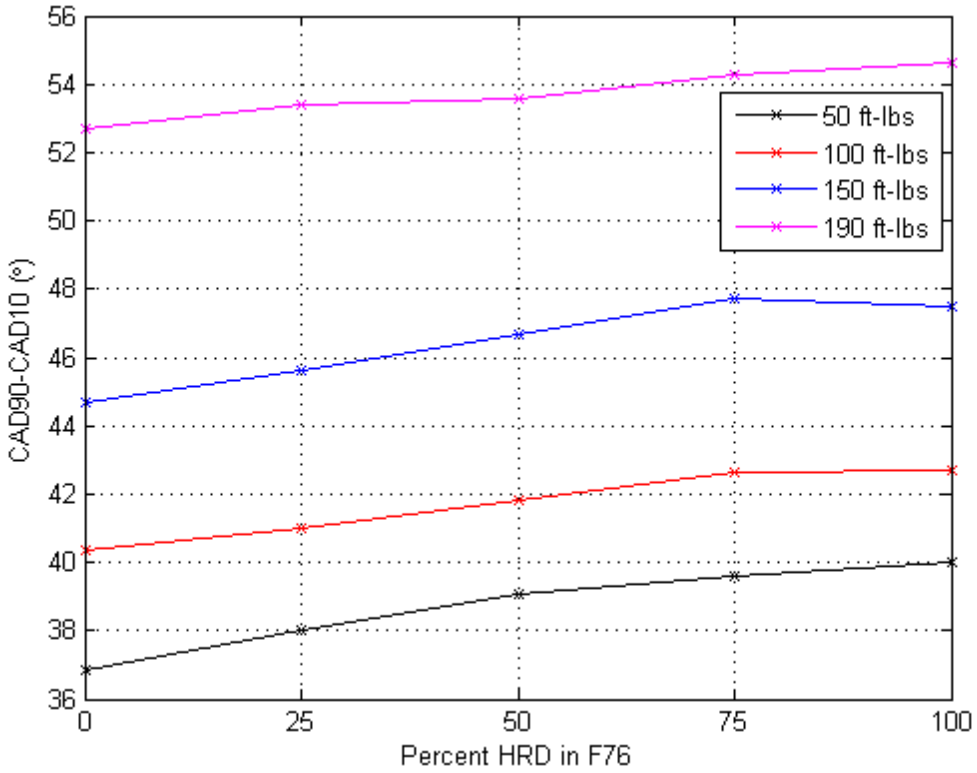

Figure 42. Combustion Duration, All Fuels at 1,650 rpm and Different Loads

I. COMBUSTION PHASING

The CP difference between HRD and F-76 is shown in Table 10 and in the contour plot of Figure 43. Figure 44 graphically displays that CP is retarded as percent HRD is increased. At 550 rpm and 50 ft-lbs no difference between HRD and F-76 was observed and the max difference in CP was 1.8 CAD at 1,650 rpm and 50 ft-lbs of torque.

Table 10. Combustion Phasing Difference (CAD): $CAD50_{HRD}$-$CAD50_{F76}$

		Load ft-lbs			
Speed rpm		50	100	150	190
	550	-0.06			
	1,100	1.47	0.85	0.87	
	1,650	1.81	0.78	0.75	0.49
	2,200		0.86	0.7	

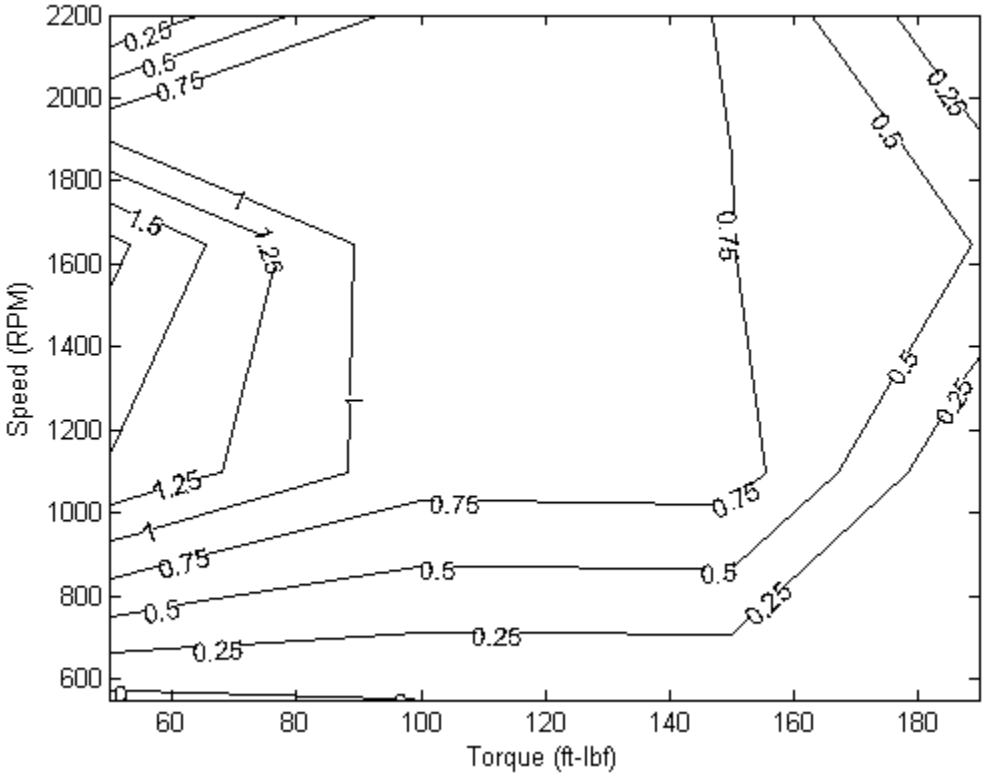

Figure 43. Combustion Phasing Difference (CAD): $CAD50_{HRD}$-$CAD50_{F76}$

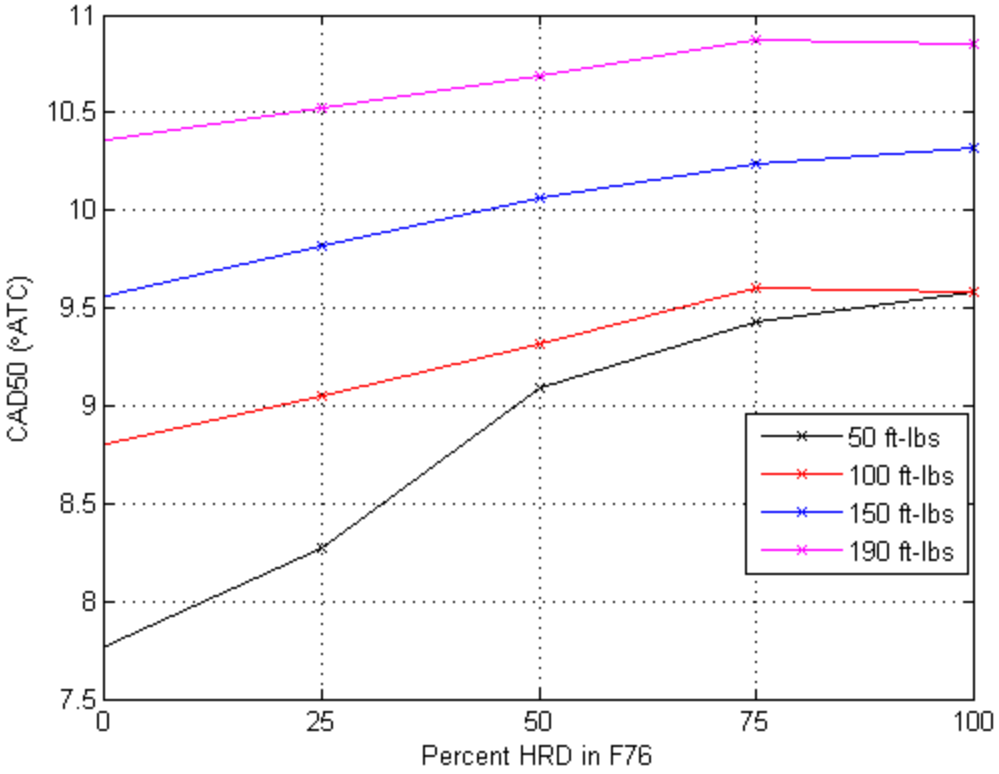

Figure 44. Combustion Phasing, All Fuels at 1,650 rpm and Different Loads

VI. CONCLUSIONS

The Detroit Diesel test engine was successfully operated on algae based HRD, F-76 and HRD/F-76 blends while combustion cycle data was recorded including cylinder pressure, crank angle position, and air-fuel flow rates.

The combustion performance metrics laid out in the thesis objectives were determined and compared between HRD and HRD/F-76 blends to F-76.

While the exact start of injection was not determined, important qualitative differences for the timing of SOI were found. As load increased SOI advanced and when speed increased SOI retarded. There was no change in SOI between the use of the different fuels allowing ignition delay to be compared.

With the much higher cetane number of HRD a shorter ignition delay than F-76 was expected and was found in this research. The maximum decrease in ignition delay for neat HRD was 2.5 crank angle degrees compared with the same operating point of F-76. This shorter ignition delay reduced the max rate of pressure rise by as much as 55% and lowered peak pressure by 6%. The angle of peak pressure was minimally affected but did show a consistent trend, slightly retarded. Combustion duration of HRD increased by as much as 8% or 3.2 crank angle degrees also due to the shorter ignition delay and slower heat release rate. Combustion phasing of neat HRD retarded slightly with the largest shift of 1.8 crank angle degrees.

HRD and HRD/F-76 blends combustion performance was comparable to F-76, suggesting good performance in engines similar to the direct injected two-stroke Detroit Diesel at NPS. In the course of testing across a wide range of speeds and loads, no evidence of any operability problems were encountered. The significant reduction in max rate of pressure rise and moderate reduction in peak pressure suggests less dynamic and maximum stresses - increasing engine life and reducing noise, beneficial to both commercial and military applications.

THIS PAGE INTENTIONALLY LEFT BLANK

APPENDIX A FUEL SYSTEM FLUSHING SOP

The following procedures were developed to standardize and ensure proper flushing of the fuel distribution system between the use of different fuels. These steps were written for the Detroit Diesel 3-53 in the Naval Postgraduate School's Marine Propulsion Lab.

Flushing the Alt Fuel Basket

1. No valves need to be switched to flush the basket
2. Drain the fuel basket and fuel/water separator
3. Connect the fuel can to the fuel line
4. Run **pumps 2 and 3** until the basket is one third full
5. Drain the basket into a waste fuel bucket

Flushing the fuel system from the Basket to the Engine

1. After flushing the Alt fuel basket, fill it half full with the fuel to be tested
2. Set **valve 5** to **Purge** and ensure the purge hose end is in the waste fuel collection bottle
3. Set **valve 4** to **Diesel 2 (Alt Purge)**
4. Set **valves 1, 2 and 3** on the fuel stand to the **Alt** fuel setting
5. Run **pump 1** until the fuel basket is one quarter full purging the fuel into the collection bottle
6. Set **valve 4** to **Alt** fuel
7. Run **pump 1** for 15 seconds
8. Drain the fuel from the basket

Now the system has been flushed and the valves are set correctly for testing a fuel from the Basket.

Flushing for Alt Fuel to Diesel 2 Tank

1. Set **valve 5** to **purge** and ensure the purge hose end is in the waste fuel collection bottle
2. Set **valve 1 and 4** to **Diesel 2**
3. Set **valves 2 and 3** to **Alt** run (this bypasses the Diesel filter)
4. Pump Diesel 2 though the system into the collection bottle for 20 seconds
5. Set **valves 2 and 3** to **Diesel 2**
6. Set **valve 5** to **Diesel 2**

Now the system has been flushed of Alt fuels and the valves are set correctly to run Diesel 2 from the outside tank.

THIS PAGE INTENTIONALLY LEFT BLANK

APPENDIX B TESTING PROCEDURES

Engine and Equipment Preparation

1. Warm up engine on Diesel 2:
    a. Oil pressure 20 psi plus or minus 5 psi
    b. Cooling water temperature state steady at 160°F
    c. Oil temperature at 150°F
2. Shut down the engine
3. After following the standard flushing procedures fill the fuel basket with the test fuel.
4. When testing the comparison between F-76 and Algae HRD the order of fuels to be tested is as follows:
    1. 100% F-76
    2. 75/25 F-76/HRD
    3. 50/50 F-76/HRD
    4. 25/75 F-76/HRD
    5. 100% HRD
5. When testing the comparison between F-76 and SPK the order of fuels to be tested is as follows:
    1. 100% F-76
    2. 75/25 F-76/SPK
    3. 50/50 F-76/SPK
    4. 25/75 F-76/SPK
    5. 100% SPK
6. Obtain data for all the points on the test matrix. Start at the lowest engine rpm and torque setting. Keep the engine rpm the same and vary the torque to gather the data for that particular rpm. Increase the rpm to the next test speed and collect data for the torque range. Continue with this procedure.
7. Ensure that all of the data collection systems are on and running properly:
    a. Synergy System
    b. LabVIEW Cylinder Pressure
    c. LabVIEW Fuel Weight
    d. Superflow WinDyn

Fuel Testing

1. Ensure fuel basket is full of test fuel and pump 1 on the fuel stand in on.
2. Start engine and run for 5 min.
3. Set engine speed and load to 550 rpm and 50 ft-lbs.

Recording Data and progressing through the Test Matrix

1. Steady engine at prescribed speed and load and record.
2. Start the fuel consumption measurement.
3. Record test cell:

a. Temperature
b. Humidity
c. Atmospheric pressure

4. Record the λ reading.
5. Record the manifold pressure.
6. Save the cycle data in the Synergy system.
7. Save cycle data in LabVIEW.
8. Once fuel consumption measurement is finished record the value.

Move on to the next speed load point.

APPENDIX C SUMMARY OF HEAT RELEASE MATLAB CODE

The following are a list of the MATLAB scripts and functions used to perform the heat release rate analysis to determine the combustion performance metrics. The entire code is stored in the NPS MPL.

ECA_analysis_loop.m – script
- ECA_input_data.xls – excel spread sheet
- ECA_analyze_one_cycle – script
  - ECA_DD3_user_icp – function. main input options
  - ECA_load
  - ECA_extract
    - ECA_int_find_np_transitions
  - ECA_channels
    - ECA_int_channel_condition
  - ECA_volume
    - slidercrank4
  - ECA_mass
  - ECA_temp
    - ECA_int_channel_condition
  - ECA_speed
  - ECA_hcv
    - ECA_int_channel_condition
  - ECA_qcv
    - ECA_int_channel_condition
  - ECA_hx_flux
  - ECA_er
    - ECA_int_channel_condition
    - ECA_int_cv
  - ECA_cycle_features
    - ECA_int_feature_find
      - ECA_int_local_max
      - ECA_int_local_min
  - ECA_avg_cycles
    - ECA_int_careful_avg

THIS PAGE INTENTIONALLY LEFT BLANK

APPENDIX D COMBSUTION TEST DATA

Fuel Type: F-76	Fuel Testing Matrix				
Date: 5-10-2013		Engine Speed [rpm]			
RmPres[in Hg]:30.09 Start Time:0617		550	1100	1650	2200
CC RefPres[psi]: 15.2 End Time:	50				
Torque [ft-lbs]	100				
	150				
	190				

Test 1		Test Cell Data	
Engine [Speed Rpm]	550	Air Temp °C	22.5
Torque [ft*lbs]	50	Rel Humidity	45.2
Crank Case Pressure [psia]	15.5	Press [in H20]	
Fuel consumption [lbs/sec]	1.19*10^-3	File name:	
Fuel time elapsed [sec]	90	λ value: 6.1	

Test 2		Test Cell Data	
Engine [Speed Rpm]	1100	Air Temp °C	23
Torque [ft*lbs]	50	Rel Humidity	45
Crank Case Pressure [psia]	16.1	Press [in H20]	
Fuel consumption [lbs/sec]	2.212*10^-3	File name:	
Fuel time elapsed [sec]	90	λ value: 7	

Test 3		Test Cell Data	
Engine [Speed Rpm]	1100	Air Temp °C	23.2
Torque [ft*lbs]	100	Rel Humidity	44.4
Crank Case Pressure [psia]	16.1	Press [in H20]	
Fuel consumption [lbs/sec]	3.044*10^-3	File name:	
Fuel time elapsed [sec]	90	λ value: 5.4	

Fuel Type: **Test 4**		Test Cell Data	
Engine [Speed Rpm]	1100	Air Temp °C	23.6
Torque [ft*lbs]	150	Rel Humidity	43.3
Crank Case Pressure [psia]	16.1	Press [in H20]	
Fuel consumption [lbs/sec]	4.297*10^-3	Run #:	
Fuel time elapsed [sec]	90	λ value: 3.65	

Test 5		Test Cell Data	
Engine [Speed Rpm]	1650	Air Temp °C	23.9
Torque [ft*lbs]	50	Rel Humidity	42.8
Crank Case Pressure [psia]	16.9	Press [in H20]	
Fuel consumption [lbs/sec]	3.137*10^-3	File name:	
Fuel time elapsed [sec]	90	λ value: 6.5	

Test 6		Test Cell Data	
Engine [Speed Rpm]	1650	Air Temp °C	24.2
Torque [ft*lbs]	100	Rel Humidity	42.5
Crank Case Pressure [psia]	16.9	Press [in H20]	
Fuel consumption [lbs/sec]	4.402*10^-3	File name:	
Fuel time elapsed [sec]	90	λ value: 5.2	

Test 7		Test Cell Data	
Engine [Speed Rpm]	1650	Air Temp °C	24.7
Torque [ft*lbs]	150	Rel Humidity	41.8
Crank Case Pressure [psia]	16.9	Press [in H20]	
Fuel consumption [lbs/sec]	5.485*10^-3	File name:	
Fuel time elapsed [sec]	90	λ value: 4	

Fuel Type: **Test 8**		Test Cell Data	
Engine [Speed Rpm]	1650	Air Temp °C	25.2
Torque [ft*lbs]	190	Rel Humidity	41.2
Crank Case Pressure [psia]	16.9	Press [in H20]	
Fuel consumption [lbs/sec]	7.779*10^-3	Run #:	
Fuel time elapsed [sec]	90	λ value: 3.0	

Test 9		Test Cell Data	
Engine [Speed Rpm]	2200	Air Temp °C	26.1
Torque [ft*lbs]	100	Rel Humidity	39.7
Crank Case Pressure [psia]	18.3	Press [in H20]	
Fuel consumption [lbs/sec]	5.78*10^-3	File name:	
Fuel time elapsed [sec]	90	λ value: 4.05	

Test 10		Test Cell Data	
Engine [Speed Rpm]	2200	Air Temp °C	26.6
Torque [ft*lbs]	150	Rel Humidity	38.5
Crank Case Pressure [psia]	18.3	Press [in H20]	
Fuel consumption [lbs/sec]	8.29*10^-3	File name:	
Fuel time elapsed [sec]	90	λ value: 3.15	

Fuel Type: 75/25 F76/HRD		Fuel Testing Matrix			
Date: 5-10-2013		Engine Speed [rpm]			
RmPres[in Hg]:30.08 Start Time:0709		550	1100	1650	2200
CC RefPres[psi]: 15.2 End Time:	50				
Torque [ft-lbs]	100				
	150				
	190				

Test 1		Test Cell Data	
Engine [Speed Rpm]	550	Air Temp °C	25.2
Torque [ft*lbs]	50	Rel Humidity	39.8
Crank Case Pressure [psia]	15.5	Press [in H20]	
Fuel consumption [lbs/sec]	0.9704*10^-3	File name:	
Fuel time elapsed [sec]	90	λ value: 6.1	

Test 2		Test Cell Data	
Engine [Speed Rpm]	1100	Air Temp °C	25.6
Torque [ft*lbs]	50	Rel Humidity	39.7
Crank Case Pressure [psia]	16.1	Press [in H20]	
Fuel consumption [lbs/sec]	1.79*10^-3	File name:	
Fuel time elapsed [sec]	90	λ value: 7	

Test 3		Test Cell Data	
Engine [Speed Rpm]	1100	Air Temp °C	23.2
Torque [ft*lbs]	100	Rel Humidity	44.4
Crank Case Pressure [psia]	16.1	Press [in H20]	
Fuel consumption [lbs/sec]	2.901*10^-3	File name:	
Fuel time elapsed [sec]	90	λ value: 5.4	

Fuel Type: **Test 4**		Test Cell Data	
Engine [Speed Rpm]	1100	Air Temp °C	26.1
Torque [ft*lbs]	150	Rel Humidity	39.4
Crank Case Pressure [psia]	16.1	Press [in H20]	
Fuel consumption [lbs/sec]	4.15*10^-3	Run #:	
Fuel time elapsed [sec]	90	λ value: 3.7	

Test 5		Test Cell Data	
Engine [Speed Rpm]	1650	Air Temp °C	26.5
Torque [ft*lbs]	50	Rel Humidity	39.2
Crank Case Pressure [psia]	16.9	Press [in H20]	
Fuel consumption [lbs/sec]	2.923*10^-3	File name:	
Fuel time elapsed [sec]	90	λ value: 6.5	

Test 6		Test Cell Data	
Engine [Speed Rpm]	1650	Air Temp °C	26.7
Torque [ft*lbs]	100	Rel Humidity	39.4
Crank Case Pressure [psia]	16.9	Press [in H20]	
Fuel consumption [lbs/sec]	4.168*10^-3	File name:	
Fuel time elapsed [sec]	90	λ value: 5.15	

Test 7		Test Cell Data	
Engine [Speed Rpm]	1650	Air Temp °C	27.1
Torque [ft*lbs]	150	Rel Humidity	38.7
Crank Case Pressure [psia]	16.9	Press [in H20]	
Fuel consumption [lbs/sec]	5.051*10^-3	File name:	
Fuel time elapsed [sec]	90	λ value: 4.1	

Fuel Type: **Test 8**		Test Cell Data	
Engine [Speed Rpm]	1650	Air Temp °C	27.5
Torque [ft*lbs]	190	Rel Humidity	38.3
Crank Case Pressure [psia]	16.9	Press [in H20]	
Fuel consumption [lbs/sec]	7.52*10^-3	Run #:	
Fuel time elapsed [sec]	90	λ value: 2.95	

Test 9		Test Cell Data	
Engine [Speed Rpm]	2200	Air Temp °C	28.1
Torque [ft*lbs]	100	Rel Humidity	37.5
Crank Case Pressure [psia]	18.3	Press [in H20]	
Fuel consumption [lbs/sec]	5.78*10^-3	File name:	
Fuel time elapsed [sec]	90	λ value: 4.10	

Test 10		Test Cell Data	
Engine [Speed Rpm]	2200	Air Temp °C	28.5
Torque [ft*lbs]	150	Rel Humidity	37.4
Crank Case Pressure [psia]	18.3	Press [in H20]	
Fuel consumption [lbs/sec]	8.135*10^-3	File name:	
Fuel time elapsed [sec]	90	λ value: 3.15	

Fuel Type: 50/50 F76/HRD		Fuel Testing Matrix			
Date: 5-10-2013		Engine Speed [rpm]			
RmPres[in Hg]:30.08 Start Time:0813		550	1100	1650	2200
CC RefPres[psi]: 15.2 End Time:	50				
Torque [ft-lbs]	100				
	150				
	190				

Test 1		Test Cell Data	
Engine [Speed Rpm]	550	Air Temp °C	26.1
Torque [ft*lbs]	50	Rel Humidity	39.3
Crank Case Pressure [psia]	15.5	Press [in H20]	
Fuel consumption [lbs/sec]	0.9426*10^-3	File name:	
Fuel time elapsed [sec]	90	λ value: 6.1	

Test 2		Test Cell Data	
Engine [Speed Rpm]	1100	Air Temp °C	26.2
Torque [ft*lbs]	50	Rel Humidity	39.3
Crank Case Pressure [psia]	16.1	Press [in H20]	
Fuel consumption [lbs/sec]	1.869*10^-3	File name:	
Fuel time elapsed [sec]	90	λ value: 7.05	

Test 3		Test Cell Data	
Engine [Speed Rpm]	1100	Air Temp °C	26.8
Torque [ft*lbs]	100	Rel Humidity	39
Crank Case Pressure [psia]	16.1	Press [in H20]	
Fuel consumption [lbs/sec]	2.787*10^-3	File name:	
Fuel time elapsed [sec]	90	λ value: 5.5	

Fuel Type: **Test 4**		Test Cell Data	
Engine [Speed Rpm]	1100	Air Temp °C	27.2
Torque [ft*lbs]	150	Rel Humidity	39
Crank Case Pressure [psia]	16.1	Press [in H20]	
Fuel consumption [lbs/sec]	4.08*10^-3	Run #:	
Fuel time elapsed [sec]	90	λ value: 3.7	

Test 5		Test Cell Data	
Engine [Speed Rpm]	1650	Air Temp °C	27.6
Torque [ft*lbs]	50	Rel Humidity	38.1
Crank Case Pressure [psia]	16.9	Press [in H20]	
Fuel consumption [lbs/sec]	2.888*10^-3	File name:	
Fuel time elapsed [sec]	90	λ value: 6.6	

Test 6		Test Cell Data	
Engine [Speed Rpm]	1650	Air Temp °C	28.1
Torque [ft*lbs]	100	Rel Humidity	37.6
Crank Case Pressure [psia]	16.9	Press [in H20]	
Fuel consumption [lbs/sec]	3.439*10^-3	File name:	
Fuel time elapsed [sec]	90	λ value: 5.15	

Test 7		Test Cell Data	
Engine [Speed Rpm]	1650	Air Temp °C	28.3
Torque [ft*lbs]	150	Rel Humidity	37.3
Crank Case Pressure [psia]	16.9	Press [in H20]	
Fuel consumption [lbs/sec]	5.732*10^-3	File name:	
Fuel time elapsed [sec]	90	λ value: 4.1	

Fuel Type: **Test 8**		Test Cell Data	
Engine [Speed Rpm]	1650	Air Temp °C	28.7
Torque [ft*lbs]	190	Rel Humidity	37
Crank Case Pressure [psia]	16.9	Press [in H20]	
Fuel consumption [lbs/sec]	7.675*10^-3	Run #:	
Fuel time elapsed [sec]	90	λ value: 2.95	

Test 9		Test Cell Data	
Engine [Speed Rpm]	2200	Air Temp °C	29.3
Torque [ft*lbs]	100	Rel Humidity	36
Crank Case Pressure [psia]	18.3	Press [in H20]	
Fuel consumption [lbs/sec]	5.68*10^-3	File name:	
Fuel time elapsed [sec]	90	λ value: 4.0	

Test 10		Test Cell Data	
Engine [Speed Rpm]	2200	Air Temp °C	29.7
Torque [ft*lbs]	150	Rel Humidity	35.4
Crank Case Pressure [psia]	18.3	Press [in H20]	
Fuel consumption [lbs/sec]	8.059*10^-3	File name:	
Fuel time elapsed [sec]	90	λ value: 3.15	

Fuel Type: 25/75 F76/HRD		Fuel Testing Matrix			
Date: 5-10-2013		Engine Speed [rpm]			
RmPres[in Hg]:30.08 Start Time:0925		550	1100	1650	2200
CC RefPres[psi]: 15.2 End Time:	50				
Torque [ft-lbs]	100				
	150				
	190				

Test 1		Test Cell Data	
Engine [Speed Rpm]	550	Air Temp °C	25.9
Torque [ft*lbs]	50	Rel Humidity	38.7
Crank Case Pressure [psia]	15.5	Press [in H20]	
Fuel consumption [lbs/sec]	0.9546*10^-3	File name:	
Fuel time elapsed [sec]	90	λ value: 6.1	

Test 2		Test Cell Data	
Engine [Speed Rpm]	1100	Air Temp °C	26.9
Torque [ft*lbs]	50	Rel Humidity	38.5
Crank Case Pressure [psia]	16.1	Press [in H20]	
Fuel consumption [lbs/sec]	1.87*10^-3	File name:	
Fuel time elapsed [sec]	90	λ value: 7.0	

Test 3		Test Cell Data	
Engine [Speed Rpm]	1100	Air Temp °C	27.4
Torque [ft*lbs]	100	Rel Humidity	38.6
Crank Case Pressure [psia]	16.1	Press [in H20]	
Fuel consumption [lbs/sec]	2.832*10^-3	File name:	
Fuel time elapsed [sec]	90	λ value: 5.4	

Fuel Type: **Test 4**		Test Cell Data	
Engine [Speed Rpm]	1100	Air Temp °C	28
Torque [ft*lbs]	150	Rel Humidity	37.6
Crank Case Pressure [psia]	16.1	Press [in H20]	
Fuel consumption [lbs/sec]	4.189*10^-3	Run #:	
Fuel time elapsed [sec]	90	λ value: 3.7	

Test 5		Test Cell Data	
Engine [Speed Rpm]	1650	Air Temp °C	28.4
Torque [ft*lbs]	50	Rel Humidity	37.2
Crank Case Pressure [psia]	16.9	Press [in H20]	
Fuel consumption [lbs/sec]	2.804*10^-3	File name:	
Fuel time elapsed [sec]	90	λ value: 6.6	

Test 6		Test Cell Data	
Engine [Speed Rpm]	1650	Air Temp °C	28.8
Torque [ft*lbs]	100	Rel Humidity	37.2
Crank Case Pressure [psia]	16.9	Press [in H20]	
Fuel consumption [lbs/sec]	3.661*10^-3	File name:	
Fuel time elapsed [sec]	90	λ value: 5.25	

Test 7		Test Cell Data	
Engine [Speed Rpm]	1650	Air Temp °C	29.1
Torque [ft*lbs]	150	Rel Humidity	36.8
Crank Case Pressure [psia]	16.9	Press [in H20]	
Fuel consumption [lbs/sec]	5.745*10^-3	File name:	
Fuel time elapsed [sec]	90	λ value: 4.15	

Fuel Type: Test 8		Test Cell Data	
Engine [Speed Rpm]	1650	Air Temp °C	29.5
Torque [ft*lbs]	190	Rel Humidity	36.1
Crank Case Pressure [psia]	16.9	Press [in H20]	
Fuel consumption [lbs/sec]	7.712*10^-3	Run #:	
Fuel time elapsed [sec]	90	λ value: 2.9	

Test 9		Test Cell Data	
Engine [Speed Rpm]	2200	Air Temp °C	30.3
Torque [ft*lbs]	100	Rel Humidity	35.3
Crank Case Pressure [psia]	18.3	Press [in H20]	
Fuel consumption [lbs/sec]	5.547*10^-3	File name:	
Fuel time elapsed [sec]	90	λ value: 4.0	

Test 10		Test Cell Data	
Engine [Speed Rpm]	2200	Air Temp °C	30.8
Torque [ft*lbs]	150	Rel Humidity	35.4
Crank Case Pressure [psia]	18.3	Press [in H20]	
Fuel consumption [lbs/sec]	8.011*10^-3	File name:	
Fuel time elapsed [sec]	90	λ value: 3.10	

Fuel Type: HRD	Fuel Testing Matrix				
Date: 5-10-2013		Engine Speed [rpm]			
RmPres[in Hg]:30.1 Start Time:1028		550	1100	1650	2200
CC RefPres[psi]: 15.2 End Time:	50				
Torque [ft-lbs]	100				
	150				
	190				

Test 1		Test Cell Data	
Engine [Speed Rpm]	550	Air Temp °C	27.7
Torque [ft*lbs]	50	Rel Humidity	36.7
Crank Case Pressure [psia]	15.5	Press [in H20]	
Fuel consumption [lbs/sec]	1.139*10^-3	File name:	
Fuel time elapsed [sec]	90	λ value: 6.15	

Test 2		Test Cell Data	
Engine [Speed Rpm]	1100	Air Temp °C	28.5
Torque [ft*lbs]	50	Rel Humidity	36
Crank Case Pressure [psia]	16.1	Press [in H20]	
Fuel consumption [lbs/sec]	1.946*10^-3	File name:	
Fuel time elapsed [sec]	90	λ value: 6.95	

Test 3		Test Cell Data	
Engine [Speed Rpm]	1100	Air Temp °C	28.8
Torque [ft*lbs]	100	Rel Humidity	36.6
Crank Case Pressure [psia]	16.1	Press [in H20]	
Fuel consumption [lbs/sec]	2.831*10^-3	File name:	
Fuel time elapsed [sec]	90	λ value: 5.4	

Fuel Type: **Test 4**		Test Cell Data	
Engine [Speed Rpm]	1100	Air Temp °C	29.3
Torque [ft*lbs]	150	Rel Humidity	36.6
Crank Case Pressure [psia]	16.1	Press [in H20]	
Fuel consumption [lbs/sec]	4.054*10^-3	Run #:	
Fuel time elapsed [sec]	90	λ value: 3.65	

Test 5		Test Cell Data	
Engine [Speed Rpm]	1650	Air Temp °C	29.5
Torque [ft*lbs]	50	Rel Humidity	36.3
Crank Case Pressure [psia]	16.9	Press [in H20]	
Fuel consumption [lbs/sec]	2.696*10^-3	File name:	
Fuel time elapsed [sec]	90	λ value: 6.6	

Test 6		Test Cell Data	
Engine [Speed Rpm]	1650	Air Temp °C	29.8
Torque [ft*lbs]	100	Rel Humidity	35.7
Crank Case Pressure [psia]	16.9	Press [in H20]	
Fuel consumption [lbs/sec]	3.654*10^-3	File name:	
Fuel time elapsed [sec]	90	λ value: 5.15	

Test 7		Test Cell Data	
Engine [Speed Rpm]	1650	Air Temp °C	30
Torque [ft*lbs]	150	Rel Humidity	36
Crank Case Pressure [psia]	16.9	Press [in H20]	
Fuel consumption [lbs/sec]	5.659*10^-3	File name:	
Fuel time elapsed [sec]	90	λ value: 4.0	

Fuel Type: Test 8		Test Cell Data	
Engine [Speed Rpm]	1650	Air Temp °C	30.4
Torque [ft*lbs]	190	Rel Humidity	35.8
Crank Case Pressure [psia]	16.9	Press [in H20]	
Fuel consumption [lbs/sec]	7.632*10^-3	Run #:	
Fuel time elapsed [sec]	90	λ value: 3.0	

Test 9		Test Cell Data	
Engine [Speed Rpm]	2200	Air Temp °C	31.2
Torque [ft*lbs]	100	Rel Humidity	35
Crank Case Pressure [psia]	18.3	Press [in H20]	
Fuel consumption [lbs/sec]	5.416*10^-3	File name:	
Fuel time elapsed [sec]	90	λ value: 4.0	

Test 10		Test Cell Data	
Engine [Speed Rpm]	2200	Air Temp °C	31.5
Torque [ft*lbs]	150	Rel Humidity	34.9
Crank Case Pressure [psia]	18.3	Press [in H20]	
Fuel consumption [lbs/sec]	8.001*10^-3	File name:	
Fuel time elapsed [sec]	90	λ value: 3.15	

THIS PAGE INTENTIONALLY LEFT BLANK

APPENDIX E SWRI FUEL DATA

SOUTHWEST RESEARCH INSTITUTE®

6220 CULEBRA RD. 78238-5166 • P.O. DRAWER 28510 78228-0510 • SAN ANTONIO, TEXAS, USA • (210) 684-5111 • WWW.SWRI.ORG

February 7, 2013

Mr. Doug Seivwright
Naval Postgraduate School
RM 206 Halligan Hall
833 Dyer Road
Monterey, CA 93943
Phone: 831-656-3580
dlseivwr@nps.edu

Re: Sample Analysis — Final Report
SwRI WO No. 66568
Revision 01 for Corrected Data

Dear Mr. Seivwright:

The fuel samples received December 10, 2012 have been analyzed as requested. The samples were received in good condition in 2.5L aluminum containers. Sample identification, test methods, and results are shown in the attached tables. Testing was conducted by January 31, 2013.

Test aliquots were taken in accordance with the test procedure. Analyses were performed in accordance with the test procedures used with no deviations or modifications. Precision should be consistent with that stated in the test procedure. The analyses pertain only to the samples received by Southwest Research Institute and represent only a sampling of a batch. This report shall not be reproduced except in full without the express written permission of Southwest Research Institute.

If you have any questions or need any further information, please call me at (210)-522-2181. We appreciate the opportunity to be of service to your firm.

Sincerely,

Mary R. Nelson

Mary R. Nelson
Senior Research Scientist
Fuels Research Laboratory
Petroleum Products Research Department
Office of Automotive Engineering

HOUSTON, TEXAS (713) 977-1377 • WASHINGTON, DC (301) 881-0226

Southwest Research Institute

Test Summary Report *for Naval Postgraduate School*

February 7, 2013

SwRI WO# 66568

DATA TABLE ATTACHED

Data Summary for the Naval Postgraduate School							
SWRI Work Order #66568							
	ProjSeq		13838	13839	13963	13964	13965
	SmplCode		DIESEL-2	SPK	BLEND1-25/75	BLEND2-50/50	BLEND3-75/25
					F-76/HRD	F-76/HRD	F-76/HRD
D1319	Aromatic	%		1			
	Olefins	%		4.7			
	Saturate	%		94.3			
D1331A	SurfTens	dynes/cm		26.8			
	TestTemp	deg C		24.5			
D2622_07	SulfAvg	PPM		16.6			
D4052M	API	.		58			
	Density	g/ml		0.7411			
	Sgravity	.		0.7469			
	TestTemp	deg C		40			
D4052M	API	.		60.1			
	Density	g/ml		0.7261			
	Sgravity	.		0.7385			
	TestTemp	deg C		60			
D4052M	API	.		62			
	Density	g/ml		0.7108			
	Sgravity	.		0.7314			
	TestTemp	deg C		80			
D4052s	API@60F			54.7			
	SPGr@60F			0.76			
	Dens@15C	g/ml		0.7598			
D445 40c	Viscosty	cSt		1.088			
D445 60C	Viscosty	cSt		0.88			
D445 80C	Viscosty	cSt		0.72			
D4809 Gross	BTUHeat	BTU/lb		20329			
	MJHeat	MJ/kg		47.285			
	CALHeat	cal/g		11293.9			
D4809 Net	BTUHeat	BTU/lb		18938			
	MJHeat	MJ/kg		44.049			
	CALHeat	cal/g		10521			
D5291 CH	Carbon	wt%		84.84			
	Hydrogen	wt%		15.25			
D613	CetaneNo		50.6	24.7	72.2	66.1	56

THIS PAGE INTENTIONALLY LEFT BLANK

LIST OF REFERENCES

[1] R. Reprice, et al. “Annual Energy Review 2011,” Energy Information Admin., DoE., Washington, DC, Rep. DOE/EIA-0384(2011), Sept. 2012.

[2] P. Holtberg, et al. “Annual Energy Outlook 2013,” Energy Information Admin., DoE., Washington, DC, Rep. DOE/EIA-0383(2013), April 2013.

[3] “Fiscal Year 2011 Operational Energy Annual Report,” DoD, Rep. 3-F901A9C, Mar. 2013.

[4] “Future Naval Fuels Program,” *Office of Naval Research*, http://www.onr.navy.mil/Science-Technology/Departments/Code-33/All-Programs/332-naval-materials/Future-Naval-Fuels.aspx (Accessed May 10, 2013).

[5] “Energy,” *U.S. Department of the Navy Energy, Environment and Climate Change*, http://greenfleet.dodlive.mil/energy/ (Accessed May 10, 2013).

[6] J. T. Bartis, and L. V. Bibber, “Alternative Fuels for Military Applications,” Internet: http://www.rand.org/pubs/monographs/MG969.html May 13, 2011.

[7] *Standard Test Method for Cetane Number of Diesel Fuel Oil*, D613a-10a, Oct. 2010.

[8] Office of Naval Research, “Fuel data on HRD and F-76,” unpublished, July 2012.

[9] K. Sugiyama, I. Goto, et al., “Effects of Hydrotreated Vegetable Oil (HVO) as Renewable Diesel Fuel on Combustion and Exhaust Emissions in Diesel Engine,” *SAE Int. J. Fuels Lubr*., vol. 5, no. 1, 2012.

[10] M. Kuronen, S. Mikkonen, P. Aakko, and T. Murtonen, “Hydrotreated Vegetable Oil as Fuel for Heavy Duty Diesel Engines,” SAE Technical Paper #2007-01-4031, 2007.

[11] H. Aatola, M. Larmi, T. Sarjovaara, and S. Mikkonen, “Hydrotreated Vegetable Oil (HVO) as a Renewable Diesel Fuel: Trade-off between NOx, Particulate Emission, and Fuel Consumption of a Heavy Duty Diesel Engine,” *SAE Int. J. Engines*, vol. 1, no. 1, 2008.

[12] P. A. Caton, S. A.Williams, R. A. Kamin, D. Luning-Prak, L. J. Hamilton and J. S. Cowart, “Hydrotreated Algae Renewable Fuel Performance in a Military Diesel Engine.” in *Internal Combustion Engine Division Spring Technical Conference*, Torino, Italy, 2012, ICES 2012-81048.

[13] R. M. Olree, D. L. Lenane, “Diesel Combustion Cetane Number Effects,” in *International Congress & Exposition*, Detroit, MI, Feb. 27- Mar. 2, 1984.

[14] J. Cowart, M. Carr, P. Caton, L. Stoulig, D. Luning-Prak, A. Moore and L. Hamilton, “High Cetane Fuel Combustion Performance in a Conventional Military Diesel Engine,” *SAE Int. J. Fuels Lubr.*, Vol. 4, pp.34-47, Apr. 2011, doi:10.4271/2011-01-0334.

[15] P. A. Caton, L. J. Hamilton, J. S. Cowart, “Understanding Ignition Delay Effects With Pure Component Fuels in a Single-Cylinder Diesel Engine,” *J. of Eng. for Gas Turbines and Power*, vol. 133, Mar. 2011.

[16] Z. S. Filipi, S. C. Homsy, K. M. Morrison, S. J. Hoffman, D. R. Dowling and D. N. Assanis, “Strain Gage Based Instrumentation for In-Situ Diesel Fuel Injection Systems Diagnostics,” presented at ASEE Annual Conf., Milwaukee, WI, 1997.

[17] “Detroit Diesel 3-53 Engine Specs,” *Barrington Diesel Club*, http://www.barringtondieselclub.co.za/353DetroitDiesel.html (Accessed May17, 2013).

[18] *Synergy Manual Operator Manual*, Ver.4.2, Hi-Techniques Inc., Madison, WI, 2011.

[19] *Detail Specification Fuel, Naval Distillate*, MIL-DTL-16884L, Oct 2006.

[20] M. A. Nelson, private communication, Feb. 2013.

[21] M. A. Nelson, “Sample Analysis SwRI WO No. 66568 Revision 01 for corrected data,” SwRI, Houston, TX, January 2013

[22] C. E. Goering, “Engine Heat Release Via Spread Sheet,” *Transactions of the ASAE*, vol. 41, no. 5, pp. 1249-1253, 1998.

[23] P. A. Caton, “Piston Power,” unpublished.

[24] J. B. Heywood, “Engine Heat Transfer,” in *Internal Combustion Engine Fundamentals*, New York, NY, McGraw Hill, 1988, ch. 12, sec. 12.4.3, pp. 680.

INITIAL DISTRIBUTION LIST

1. Defense Technical Information Center
   Ft. Belvoir, Virginia

2. Dudley Knox Library
   Naval Postgraduate School
   Monterey, California